



Published in final edited form as:

Behav Brain Res. 2023 February 02; 437: 114106. doi:10.1016/j.bbr.2022.114106.

Paired Associates Learning is Disrupted After Unilateral Parietal Lobe Controlled Cortical Impact in Rats: A Trial-by-Trial Behavioral Analysis

Samantha M. Smith^{1,3}, Elena L. Garcia¹, Caroline G. Davidson¹, John J. Thompson¹, Sarah D. Lovett¹, Nedi Ferekides¹, Quinten Federico¹, Argyle V. Bumanglag¹, Abbi R. Hernandez⁴, Jose F. Abisambra^{1,5}, Sara N. Burke^{1,2,*}

¹Department of Neuroscience, University of Florida College of Medicine, Gainesville, FL

²Institute on Aging, University of Florida, Gainesville, FL

³Graduate Program in Biomedical Sciences, Neuroscience Concentration, University of Florida

⁴Department of Medicine; Division of Gerontology, Geriatrics, and Palliative Care, University of Alabama at Birmingham, Birmingham, AL

⁵Center for Translational Research in Neurodegenerative Disease, University of Florida College of Medicine, Gainesville, FL

Abstract

*Indicates corresponding author, **Correspondence should be addressed to:** Sara N. Burke, PhD, Department of Neuroscience, University of Florida, P.O. Box 100244, Gainesville, FL 32611; Tel. +1 (352) 294-4979; Fax: +1 (352) 392-8347; burkes@ufl.edu.

Author Contributions:

SMS collected data, contributed analytic tools, analyzed data, and wrote the manuscript. ELG collected and analyzed data, CGD collected and analyzed data, JJT collected data, SDL performed the surgeries, NF collected and analyzed data, QF collected data, AVB helped oversee and perform research, ARH helped with experimental design and performed research, JFA and SNB designed the research and edited the manuscript.

Publisher's Disclaimer: This is a PDF file of an article that has undergone enhancements after acceptance, such as the addition of a cover page and metadata, and formatting for readability, but it is not yet the definitive version of record. This version will undergo additional copyediting, typesetting and review before it is published in its final form, but we are providing this version to give early visibility of the article. Please note that, during the production process, errors may be discovered which could affect the content, and all legal disclaimers that apply to the journal pertain.

Conflict of Interest

Authors report no conflict of interest.

CRediT authorship contribution statement

Samantha M. Smith, lead author. Software, Formal analysis, Investigation, Data curation, Writing, Review and Editing, Visualization, Project Administration

Elena L. Garcia, Formal analysis, Investigation, Writing, Visualization

Caroline G. Davidson, Formal analysis, Writing, Visualization

John Thompson, Investigation

Sarah D. Lovett, Investigation

Nedi Ferekides, Investigation, Formal Analysis, Visualization

Quinten Federico, Investigation

Argyle V. Bumanglag, Supervision

Abbi R. Hernandez, Investigation, Review and Editing, Visualization, Project administration and Execution

Jose F. Abisambra, Conceptualization, Resources, Review and Editing, Funding Acquisition

Sara N. Burke, corresponding author. Conceptualization, Methodology, Resources, Review and Editing, Project Administration, Funding acquisition

Approximately 60-70 million people suffer from traumatic brain injury (TBI) each year. Animal models continue to be paramount in understanding mechanisms of cellular dysfunction and testing new treatments for TBI. Enhancing the translational potential of novel interventions therefore necessitates testing pre-clinical intervention strategies with clinically relevant cognitive assays. This study used a unilateral parietal lobe controlled cortical impact (CCI) model of TBI and tested rats on a touchscreen-based Paired Associates Learning (PAL) task, which is part of the Cambridge Neuropsychological Test Automated Battery. In humans, the PAL task has been used to assess cognitive deficits in the ability to form stimulus-location associations in a multitude of disease states, including TBI. Although the use of PAL in animal models could be important for understanding the clinical severity of cognitive impairment postinjury and throughout intervention, to date, the extent to which a rat model of TBI produces deficits in PAL task performance has not yet been reported. This study details the behavioral consequences of the CCI injury model with a Trial-by-Trial analysis of PAL performance that enables behavioral strategy use to be inferred. Following behavior, the extent of the injury was quantified with histology and staining for the presence of glial fibrillary acid protein and ionized calcium-binding adapter molecule 1. Rats that received unilateral CCI were impaired on the PAL task and showed more aberrant response-driven behavior. The magnitude of PAL impairment was also correlated with Iba1 staining in the thalamus. These observations suggest that PAL could be useful for pre-clinical assessments of novel interventions for treating TBI.

Keywords

traumatic brain injury; CANTAB; hippocampus; thalamus; response-bias; neuroinflammation

1. INTRODUCTION

Traumatic brain injury (TBI) in the U.S. continues to be a leading cause of disability for minors and young adults (CDC, 2022). Moreover, the rate of emergency department visits for TBI in individuals over 65 has increased by 78% from 2002 to 2017 (Cusimano et al. 2020). Acute effects of TBI can range from dizziness, nausea, headaches, and memory loss to motor coordination deficits, vision impairment, anxiety, irritability, and depression. Unfortunately, many individuals with TBI will also suffer from chronic neurocognitive symptoms that can lead to a decreased quality of life (McAlliser & Arciniegas 2002; Quinn et al. 2018). TBI occurs in two phases, the first of which is mechanical damage that occurs from the force of impact. The second phase of injury can occur in the days to weeks following initial insult and results from inadequately understood molecular cascades that often lead to the death of healthy and undamaged cells (Borgens & Liu-Snyder 2012). Due to the complexities of this secondary injury and the diverse array of cognitive dysfunction seen following TBI, animal models continue to be imperative in biomedical research aimed at understanding and treating TBI.

A promising avenue for the study of rat TBI models is the ability to monitor intervention outcomes in a clinically relevant setting. In humans, paired associates learning (PAL) is a touchscreen-based cognitive assessment within the Cambridge Neuropsychological Test Automated Battery (CANTAB) (Robbins et al. 1994, 1998; Barnett et al. 2016).

Performance on PAL correlates with structural brain damage in individuals with TBI (Newcombe et al. 2016) and has been used in clinical trials testing the safety and efficacy of the cholinesterase inhibitor rivastigmine in TBI patients with memory impairment (Silver et al. 2006, 2009). Additionally, PAL was first developed and used in nonhuman primates (Weed et al. 1999; Taffe et al. 2002) and has since been modified for use in rats (Bussey et al. 2008; Talpos et al. 2009). The cross-species translational power of the touchscreen-based PAL task presents the ability to enhance the preclinical to clinical biomedical research pipeline. Despite the increasing imperative to conduct preclinical intervention testing that more closely reflects that seen in humans, *no studies have yet detailed the extent to which a rat CCI-model of TBI leads to behavioral deficits in PAL performance that mirror those seen in human patients.*

In rats, successful completion of the PAL task requires associative learning to accurately pair a stimulus (flower, plane, or spider) with its correct location on the touchscreen (left, center, or right). While these object-place associations are known to require the hippocampus (HPC; Talpos et al. 2009; Kim et al. 2015; Langston et al. 2010; Yoon et al. 2012), the PAL task also likely involves structures relating to visual stimulus recognition, selective attention, executive control, and behavioral flexibility, all of which are commonly disrupted following TBI. The current study assessed performance on PAL after unilateral controlled cortical impact (CCI) to the parietal lobe of adult male and female rats. *This study used MATLAB-assisted analysis scripts to evaluate PAL performance in a trial-by-trial (TxT) format across 90-trial testing sessions to more thoroughly examine the cognitive deficits that occurred due to the injury paradigm. Automated touchscreen-based testing chambers collect a vast array of data related to behavioral performance, and researchers will benefit from analyses which leverage this data. The scripts used for our TxT analyses are uploaded to GitHub (see methods) to facilitate other researcher's endeavors in conducting these behavioral analyses for the PAL task.* After the completion of cognitive testing, post-mortem histology was conducted to understand the extent of spared tissue in our model resulting from injury as well as the presence of glial fibrillary acid protein (GFAP) and ionized calcium-binding adapter molecule 1 (IBA1) in 12 regions of interest around the injury site. Furthermore, principal component analysis was performed to reduce the dimensionality of the dataset and inform how the various behavioral and histological measures were correlated with one another to aid future studies that use the PAL task in translational research for TBI treatment.

2. METHODS

2.1 Rats

A total of 16 adult (two months at time of arrival; n=8 male, n=8 female) Long Evans rats from Charles River were used in this study. *Prior to completion of the study, three rats assigned to the sham condition and one rat assigned to the injury condition died from health complications unrelated to the CCI injury model (Sham: two female, one male; Injury: one female). Two of these deaths occurred prior to surgery, and two occurred post-surgery.*

Each rat was housed individually in a standard Plexiglas cage and maintained on a 12-hour reversed light/dark cycle (lights off at 8:00 am). Testing was conducted exclusively

in the dark phase of the cycle. Rats were given one week to habituate to the facility prior to behavioral testing or food restriction with *ad libitum* access to food (standard rat maintenance diet) and water. Throughout this habituation period, rats were handled daily. Upon the initiation of training, food was restricted to maintain the rats 80-85% of their normal baseline body weight and had *ad libitum* access to water. Baseline weight was considered the weight at which an animal had an optimal body condition score of 3.0. Throughout the period of restricted feeding, rats were weighed daily, and body condition was assessed and recorded weekly to ensure a range of 2.5-3.5. The body condition score was assigned based on the presence of palpable fat deposits over the lumbar vertebrae and pelvic bones (Ullman-Culleré & Foltz, 1999; Hickman & Swan, 2010). Rats with a score under 2.5 were given additional food to promote weight gain. Food was provided *ad libitum* for the week following surgery. All procedures were conducted in accordance with the National Institutes of Health guidelines and were approved by the Institutional Animal Care and Use Committees at the University of Florida.

2.2 Surgery

Rats were pseudo-randomly selected, counterbalancing for sex, for either the TBI (n = 4 males/4 females), or sham (n = 4 males/4 females) condition prior to beginning behavioral testing. *After completing all touchscreen shaping and reaching a preset criterion performance on the PAL task, rats were taken for surgery. At the time of impact, all rats were between 3-5 months of age.* Initial anesthesia was induced by placing rats into a vented anesthesia chamber with 5% isoflurane. The head was shaved and then rats were placed in a stereotaxic frame and anesthesia was maintained with a nose cone at 1.5-2% isoflurane. Utilizing aseptic technique, a midline incision was made to expose the skull. A 7 mm diameter craniotomy was made, centered at AP -4.5 and ML + 4.5, targeting the rats' right parietal lobe, as depicted in Figure 1A. A controlled cortical impact (CCI) was performed for rats in the experimental condition. The impact was delivered by a pneumatic piston (Model PCI3000 PinPoint Precision Cortical Impactor, Hatteras Instruments) containing a 5 mm diameter tip, which delivered a force at the rate of 4m/second, a 3mm compression and a 100ms dwell time Following the impact, the bone flap was replaced with bone wax, the incision was sutured, and rats were allowed to recover from anesthesia. Sham condition rats underwent similar surgical procedures but did not undergo a cortical impact. Rats had *ad libitum* access to food and water for seven days following surgery before returning to food restriction and PAL testing. Meloxicam injection (Alloxate; 5 mg/kg) was given before surgery and every 24 hours after surgery for 48 hours. After surgery, buprenorphine (Buprenex; 0.03 mg/kg) was administered every 8-12 hours for 24 hours, and rats received 0.5 ml of liquid antibiotic (Sulfamethoxazole and trimethoprim combination) with their food for 7 days. Rats were monitored post-surgery until time of sacrifice for any signs of distress. All procedures were conducted in accordance with the National Institutes of Health guidelines and were approved by the Institutional Animal Care and Use Committees at the University of Florida.

2.3 Testing Chambers and Touchscreen Shaping

All shaping and testing procedures were conducted in standard Bussey-Saksida rat touchscreen chambers (Horner et al. 2013) purchased from Lafayette Instruments (Lafayette,

IN) that were housed within soundproof boxes. Engaging with the touchscreen apparatus requires a nose-poke on the correct stimulus on the screen to elicit a liquid reward of flavored nutritional shake delivered by a magazine port. *Rats were shaped to use the touchscreens through 5 incremental training stages: Magazine, Any Touch, Must Touch, Must Initiate, and Punish Incorrect. Magazine training introduced the rats to liquid reward when the magazine opening was nose poked. After the reward was collected, the next trial began after a 10-second inter-trial interval. Any Touch introduced the rats to reward when they touched anywhere on the touchscreen. Must Touch introduced the rats to reward only when they touched specific panels. Must Initiate introduced the rats to reward only after they touched specific panels on the screen after initializing a trial with a nose poke in the magazine opening. Finally, Punish Incorrect introduced the rats to a house light if an incorrect choice was made. Criterion for all 5 stages of shaping was 2 days completing 90 trials in 45 minutes or less.*

After rats had completed all stages of the shaping protocol, they were moved on to the PAL Acquisition task. During the PAL Acquisition task, subjects were tested on an unpunished version of PAL where only the correct selection would initiate a reward, but incorrect choices were not punished, and the stimuli remained on the screen until the correct choice was made. The criterion for the PAL Acquisition was two consecutive days of 90 trials or 180 trials total, at which point rats advanced to the full task.

2.4 PAL & iPAL

The rodent PAL and iPAL tasks are designed to assess associative learning of a stimulus with a location (i.e., flower is associated with the left). Associative learning is known to require the hippocampus (Suzuki 2007, Talpos et al., 2009; Kim et al., 2015), and may be sensitive to cognitive decline in several contexts (Kramer et al. 2009; Lee et al. 2013; Diwadkar et al. 2008; Collie et al. 2002). The PAL task is part of the Cambridge Neuropsychological Test Automated Battery. In humans, PAL has been used to assess cognitive deficits in the ability to form stimulus-location associations in a multitude of disease states, including TBI. During the rodent PAL task, rats are required to nose poke the stimulus (flower, plane, spider) being presented in its correct location (left, middle, right) to receive a food reward. During a trial, two stimuli are presented at the same time; one stimulus is presented in the correct location and the other in the incorrect location. The unused, third location of a given trial is a blank panel and any engagement with this blank panel does not elicit any change in the environment (no reward or house light). Each of the three stimuli are assigned to a correct location that is unique to the stimuli, resulting in six different trial types. The iPAL task is a modification of PAL in which a novel image (a white maple leaf) is presented in the blank panel as an irrelevant distractor. Selection of the novel stimulus did not elicit a reward and was therefore considered an incorrect choice. The PAL task assesses associative learning, but the iPAL task assesses associative learning in addition to testing susceptibility to distraction. This additional behavioral measure in our study allowed us to measure whether the rats exhibited executive dysfunction as measured by tendency to perseverate on a novel, task-irrelevant stimulus. For more detail regarding the PAL and interference (i)PAL tasks as well as the shaping parameters used to accustom the rats to the touchscreen chambers, please see Smith, Zequeira et al. (2022).

Rats were trained to complete 90 trials in a daily session within 45 minutes during shaping. Each PAL and iPAL session lasted for a maximum of 45 minutes or concluded upon completion of 90 trials. The trials were pseudorandomly presented to ensure that no specific trial type was presented more than 3 consecutive times. In our PAL and iPAL protocols, rats started their daily session by engaging with the magazine chamber for a 'pre-reward.' After the reward was collected, the first trial began after a 10-second inter-trial interval (ITI) in which another trial could not be initiated. This ITI was standard across all 90 trials within a testing session. If an incorrect selection was made during the PAL or iPAL tasks, no reward was received, and the 10-second ITI occurred with the house light turning on. Rats were tested on the PAL task until they reached a criterion performance of 83.33% correct for two consecutive testing days. After completion of criterion on PAL, rats underwent CCI surgery. Following recovery, rats were re-tested on PAL until criterion performance was again met. Once criterion on PAL was met post-surgery, rats then moved on to complete 12 days of iPAL testing before sacrifice and postmortem histology. Figure 1 depicts the timeline of the experimental procedures detailed above, a schematic of a rat completing a trial in the touchscreen environment, and the 6 possible PAL and iPAL trial types denoted with a green square to indicate the correct selection on each trial type.

2.5 Trial-by-Trial Behavioral Measures

We created a series of analysis scripts to leverage the data collected during the PAL task in our automated testing chambers. Specifically, we inferred whether rats used different learning strategies prior to meeting criterion performance on PAL using TxT analytical approaches that looked at behavior within a 90-trial daily session and across session days. These approaches were implemented using MATLAB scripts to automatically gather variables of interest using the raw data output from the testing chambers. These scripts are available at the following GitHub repository link: (<https://github.com/BurkeMaurer-Lab/PAL-TxT-Scripts.git>) along with the raw touchscreen data from this study.

Stimulus and location bias.—One potential strategy a rodent may exhibit is to base its selection on a single feature parameter (either the selection's location or its identity) without considering the stimulus-location association required for successful completion of PAL. Rodents may have biases toward the following selections in the PAL task: the plane, flower, or spider (stimulus bias); or the left, middle, or right panels of the touchscreen chamber itself (location bias). If persistent, this stimulus or location bias would interfere with task acquisition. A stimulus bias index was therefore calculated for each individual stimulus (plane, spider, and flower) and location (left, middle, right). An absolute bias for an individual stimulus would be 1 and no bias for an individual stimulus would be 0. The total bias index was then calculated by adding up the 3 individual biases. The location bias index was calculated in the same way using location on the screen (left, center, right) as the feature parameter.

Win-stay and lose-shift strategies.—Another potential strategy that could be used during PAL testing is the implementation of reward heuristics, where the choice selection on a trial is a function of the reward or lack thereof received on the immediately preceding trial. In this regard, rats could choose to adopt a win-stay strategy to stay with selecting

a previously rewarded feature (either stimulus or location) without considering the stimulus-location association on the current trial. For example, the selection of the flower in the left location resulted in a reward on one trial. Thus, on the subsequent trial the animal selects the left location even though the plane is in this location and that is an incorrect response. They may also adopt a lose-shift strategy. The use of win-stay and lose-shift strategies were calculated as the total number of times a strategy was used / total number of times a strategy was possible. For each of the 4 possible strategies, stimulus win-stay, stimulus lose-shift, location win-stay, location lose-shift, the maximal bias is 1, with 0 indicating that the strategy was not used at all. These calculations included the presentation of pseudorandom duplicate trials and trials in which the win-stay or lose-shift strategies resulted in the correct response.

Maintenance of associations across test day.—To assess whether the injured rats were impaired on PAL because of forgetting the stimulus-location associations formed during the previous day's session, average percent correct by discrete trial blocks was calculated and compared within and between daily test sessions. The 90 trials were divided into 2 blocks of 45 trials and percent correct was calculated for each individual block of trials. A decline in performance between the last 45 trials 1 day and the first 45 trials of the subsequent testing day would be evidence of forgetting and an inability to maintain the newly formed associations.

2.6 Histological Analysis

Rats were transcardially perfused with 4% paraformaldehyde in phosphate buffered saline after completion of behavioral testing. *Due to the nature of the PAL task occurring across weeks to months, the rodents varied in the time it took to finish all testing. This means that this study did not have consistent endpoints following time of injury; rather, endpoints were consistent with regard to behavioral performance and the completion of testing. As such, all rodents used in this study were sacrificed between 45 and 57 days after receiving CCI or sham surgery. Furthermore, the rats arrived at the housing facility at 2 months old, were injured between 3-5 months and sacrificed between 4.5-6.5 months.* Brains were post-fixed for 24 hours and sliced into 50-micron thick sections using a vibratome. Each microscopy slide was plated with sequential slices approximately 350 microns apart. Sections were Nissl stained (1% Cresyl Violet) for lesion volume analysis. *Tissue was also stained for the presence of GFAP and IBA1 epitopes. GFAP is an intermediate filament protein expressed by astrocytes in the central nervous system that has been viewed as an index of gliosis and correlate of neural damage (Finch 2003; Hausmann, 2003). IBA1 is a calcium-binding protein in microglia and macrophages that is involved in phagocytosis in activated microglia (Ohsawa et al. 2004). As microglia move to an activated state after exposure to pathogen and damage-associated molecular patterns (Jurga, Paleczna, & Kuter 2020), this protein is associated with pro-inflammatory processes. While these markers do not provide sufficient analysis of inflammatory response to TBI nor justify the mechanisms that are responsible for the deficits seen in the PAL task, we employed these measures to get basic information regarding the state of the brain in relation to the behavioral deficits. Future behavioral studies would benefit from less dated markers of astrocytes, microglia, and macrophages.*

For the GFAP and IBA1 immunohistochemistry, primary antibody was used at [1:10,000] for GFAP (GA5 mAb #3670; Cell Signaling Technology) and at a [1:10,000] for IBA1 (ab107159; Abcam). Secondary antibody was used at [1:2,000] for GFAP (rabbit antimouse biotinylated; ab107159; Abcam) and [1:2,000] for IBA1 (rabbit anti-goat biotinylated; ab64257). Sections were mounted on Superfrost Plus slides, air dried, and placed in 0.1 M Tris buffer, pH 7.6 (Tris). Slides were then immersed in 85– 87°C Tris for 1 minute, washed in Tris, and placed in Tris containing 0.25% bovine serum albumin (BSA; fraction V; Sigma) and 0.1% Triton X-100. After primary antibody incubation, slides were washed in Tris-BSA-Triton X buffer, pH 7.6 (2-5 minutes minimum). Slides were incubated in secondary antibody solution in TrisBSA-Triton X buffer for 2 hours, washed in the same buffer, and then incubated for 2 hours in avidin-biotinHRP complex (PK-6100; Vector Laboratories ABC Elite Kit diluted [1:1,000] in TrisBSA-Triton X buffer). Slides were then washed in Tris (3-5 minutes minimum) and incubated in a hydrogen peroxide-generating 3-3'-diaminobenzidine (DAB) solution (100 ml Tris containing 50 mg DAB, 40 mg ammonium chloride, 0.3 mg glucose oxidase, and 200 mg β -D-glucose). After incubation in DAB solution (20–30 minutes), slides were rinsed in Tris, dehydrated in graded ethanols and xylene, and cover slipped with Permount mounting medium. Brightfield images were acquired on a Keyence BZ-X800 microscope (Keyence Corporation of America, Itasca, IL).

For semi quantitative analysis of the GFAP & IBA1 stains, 12 regions of interest were identified, depicted in Figure 2A. Five regions of interest were defined a priori within the hippocampus due to the high degree of involvement of this structure required for the cognitive testing used in this study: proximal CA1 (p.ca1), CA1, subiculum (sub), CA3, and CA3c area (CA3c). Seven additional thalamic regions were later identified for inclusion: lateral posterior nucleus - mediorostral part (lpmr), lateral dorsal nucleus - ventrolateral part (ldvl), posterior nuclear group (po), ventral posteromedial nucleus (vpm), ventral posterior lateral nucleus (vpl), mediodorsal nucleus – medial part (mdm), and mediodorsal nucleus – lateral part (mdl). The optical density in these regions of interest was quantified across three slices for each animal in each hemisphere. Images of the DAB-stained sections were first captured at 10X magnification. In FIJI (NIH, Bethesda MD), the images were color deconvoluted and converted into 8-bit grayscale. A pre-designed set of ROIs with standard sizes were utilized. For each slice, experimenters blinded to condition identity adjusted the ROI boxes to best match the tissue's own anatomical features. After calibrating the Measure function to an optical density standardization image, an optical density curve was created for use in measuring each ROI. Within-slice ROI measurements were normalized by the mean gray value of that slice to account for variability in tissue darkness.

For spared tissue volume analysis, eight representative Nissl-stained sections across the extent of injury were imaged on a Keyence (BZ-X800) at 2X magnification. Using the Hybrid Cell Count module in the BZ-X800 Analyzer software, the area (μm^2) of each hemisphere was recorded, as well as that of the ipsilateral hippocampus and cortex (dorsal to rhinal sulcus), the latter two being hand-traced by a blinded experimenter as depicted in Figure 2B. Ipsilateral hemisphere, hippocampal, and cortical measurements were normalized by the slices' contralateral hemisphere to mitigate between subject variability in brain size.

2.7 Analytical & Statistical Parameters

All TxT analyses were conducted using custom written code (MATLAB, MathWorks Inc, R2021A) that is available at <https://github.com/BurkeMaurer-Lab/PAL-TxT-Scripts.git>. For an in-depth discussion of all TxT PAL analyses, please see Smith, Zequeira et al. (2022). Stimulus and location biases were calculated as follows for each feature (stimulus or location) separately:

$$\frac{\text{total number of choices(maximum 60)} - \text{total number of correct responses for that feature(maximum of 30)}}{\text{total number of correct responses for that feature(maximum of 30)}}$$

The bias was calculated for each image or location and then summed across the 3 stimuli of the same dimension (plane bias + spider bias + flower bias = total stimulus bias, or left bias + central bias + right bias = total location bias). Bias values ranged from 0 (no bias) to 2 (absolute bias).

Win-stay and lose-shift strategies were calculated as total number of times a strategy was used / total number of times a strategy was possible. For each of the 4 possible strategies (stimulus win-stay, stimulus lose-shift, location win-stay, and location lose-shift), strategy index ranged from 0 (no use of strategy) to 1 (maximal use of strategy). Statistical analyses were performed using the statistical software R.3.6.3. Whenever possible, we elected to fit a mixed effects linear model using the R package “lme4” (version 1.1-28; <https://github.com/lme4/lme4/>) to assess statistical significance due to the limitations of ANOVA in considering variability between subjects (Barr et al. 2013; Brown, 2021), especially for repeated measures designs in which both within and between subjects’ variables are present. P-values < 0.05 were considered statistically significant. Bonferroni corrections were used for multiple comparisons. Reporting of the linear model effects in this manuscript follow Satterthwaite’s method (Giesbrecht & Bums 1985; Kuznetsova, Brockhoff, & Christensen 2017). When appropriate, behavioral data were analyzed by T-tests with correction for unequal variances if necessary. The choice of statistical test was based on assumptions of normality, assessed with the Shapiro-Wilk test and with Levene’s test.

3. RESULTS

3.1 PAL Performance

To assess post-surgical PAL performance, a linear mixed effects model (LMEM) was fit to predict percent correct with both condition (sham or injury) and day as fixed effects. The model also included the individual rats as a random effect. Although some rats completed more than 12 days of PAL testing, all rats only completed 12 days of iPAL testing. For consistency of reporting, all LMEM analyses are across 12 days of PAL testing. The model’s power was substantial with a conditional R^2 value of 0.63 and a marginal R^2 of 0.22. The model’s intercept was 78.55 (95% CI [71.63, 85.47], $T_{(138)} = 22.44$, $p < .001$). This model found significant main effects of condition ($F_{(1,15.45)} = 7.157$, $p = 0.02$) and day ($F_{(1,130)} = 4.059$, $p = 0.046$), as well as a significant day by condition interaction ($F_{(1,130)} = 6.067$, $p = 0.015$). Specifically, all rats showed improved PAL accuracy following surgery, but the TBI group performed worse overall and showed a slower rate of increasing accuracy over days

than did the control animals. Figure 3A shows the average percent correct of each condition on the day before surgery as well as the first 12 days of testing after recovery from surgery. *When sex was added to the model, it did not explain any additional variance ($F_{(1,11.44)} = 0.017$, $p = 0.898$, standardized $\beta = -0.02$), suggesting that there were not observable sex differences in PAL task performance. Since it is impossible to prove the absence of an effect, a power analysis was run to determine the number of animals that would be required to reject the null hypothesis of no sex differences in PAL performance with an 80% probability. This power analysis indicated that the necessary sample size would need to be 198 animals per group.* Further post hoc T-tests found that before surgery, both conditions performed at similar levels on PAL ($T_{(10)} = 0.292$, $p = 0.775$). Post-surgery, the first five days of PAL performance was statistically different between the groups ($T_{(10)} = 2.378$, $p = 0.039$); Figure 3B. Figure 3C shows the cumulative error prior to reaching criterion on PAL post-surgery. The sham condition had an average of 223.2 ± 44.94 S.E.M. errors across testing. The injury condition had 317.2 ± 27.43 S.E.M. An unpaired t-test did not reach statistical significance ($T_{(10)} = 1.894$, $p = 0.088$), although there was a trend for the CCI treated rats to make more errors. Overall, the data presented in Figure 3A–C indicates that rats that received CCI were less accurate on PAL following surgery compared to sham rats and required more time to return to criterion performance.

To rule out whether differences in motor coordination or motivation may have affected performance between the conditions, we fit a LMEM for trial latency (time between the start of a new trial and when a decision is made, in seconds). Figure 3D shows the average latency for each condition across the first 8 days of testing post injury. This model found a significant main effect of day ($F_{(1, 124.9)} = 13.89$, $p = 0.0003$) but not condition ($F_{(1,36.87)} = 0.373$, $p = 0.545$). Furthermore, the day by condition interaction was also nonsignificant ($F_{(1,124.7)} = 0.258$, $p = 0.613$). These results suggest that there was no difference in trial latency between the conditions, making it unlikely that any potential motor deficits in the injury condition affected performance on PAL. Furthermore, the finding that both conditions' latencies increased across testing day indicates that motivation increased with the learning and familiarity of the task regardless of injury condition, which was expected with similar levels of motivation across conditions.

In addition to the accuracy and latency measures detailed above, the PAL task presents the ability to run a TxT analysis of performance measures across a 90-trial session. For these TxT analyses, we first looked at trial blocks over the course of a session across testing days to understand if the two conditions of rats diverged in terms of performance in earlier vs. later trials in a session. This was achieved through blocking the daily 90-trial sessions into two blocks of 45 trials and taking the difference between the percent correct values in these epochs. We then fit a LMEM. This model found no significant effects of day, condition, or day by condition interaction (day: $F_{(1, 128.2)} = 0.944$, $p = 0.333$, condition: $F_{(1,46.84)} = 0.278$, $p = 0.601$, day by condition: $F_{(1,128.1)} = 0.0054$, $p = 0.941$) suggesting that both conditions had similar trajectories of performance in early and late trials. The addition of sex to the model did not account for any additional variance seen in block performance ($p > 0.05$, $\beta < 0.1$). These null results are not depicted in graphical format.

The next TxT analysis we conducted was a bias index for feature parameter selections during a testing session. Bias is the tendency for a rat to default to a response-driven behavior, choosing a single feature parameter repeatedly. In the case of PAL, bias can be towards a certain location (for example, choosing the left panel repeatedly even when incorrect), or a certain stimulus (for example, choosing flower repeatedly regardless of its location). Figure 3E and 3F shows the average bias by condition on the day before surgery and across 12 days of testing post-surgery for stimulus and location features, respectively. For stimulus bias, LMEM found a significant main effect of condition ($F_{(1,19,29)} = 6.415$, $p = 0.020$) as well as a significant condition by day interaction ($F_{(1,130)} = 7.380$, $p = 0.008$), with injured rats showing larger stimulus bias that was more persistent over days. Day alone was non-significant ($F_{(1,130)} = 1.316$, $p = 0.2534$). Similarly, for location bias, LMEM found a significant main effect of condition ($F_{(1,17,87)} = 11.08$, $p = 0.004$) and condition by day interaction ($F_{(1,130)} = 15.30$, $p = 0.00015$), while day alone was non-significant ($F_{(1,130)} = 0.547$, $p = 0.461$). Again, the injured rats showed a greater location bias relative to control rats that persisted over days. These results suggest that the CCI-injured rats exhibited higher response biases for both stimulus and location features across testing than sham rats, which likely contributed to their overall performance deficit as this bias has been shown previously to negatively correlate with percent correct (Smith, Zequeira et al. 2022).

In addition to having a response-driven bias, rats could also adopt an outcome-based strategy. On a given trial, they could either select a previously rewarded feature (win-stay) or switch from a previously unrewarded feature (lose-shift). For example, if a rat incorrectly chooses the flower in a trial and is then immediately given another trial where flower is now correct, if the rat then does not choose flower, this can be considered a stimulus lose-shift strategy. A strategy usage index was calculated for four outcome-based heuristics in PAL before and after surgery: stimulus win-stay, location win-stay, stimulus lose-shift, and location lose-shift. On the day before surgery, all strategy use was the same for both surgery conditions (stim ws: $T_{(10)} = 0.078$, $p = 0.9394$; loc ws: $T_{(10)} = 0.128$, $p = 0.901$; stim ls: $T_{(10)} = 0.762$, $p = 0.464$; loc ls: $T_{(10)} = 0.261$, $p = 0.799$). After injury, stimulus win-stay, location win-stay, & location lose-shift did not significantly differ by condition ($F_{(1,83,763)} = 3.794$, $p = 0.055$; $F_{(1,68,039)} = 1.991$, $p = 0.163$; $F_{(1,140)} = 1.250$, $p = 0.2655$). Stimulus lose-shift, however, had a significant condition ($F_{(1,45,947)} = 7.417$, $p = 0.009$) and condition by day ($F_{(1,130)} = 4.593$, $p = 0.034$) interaction. The effect of day alone did not reach significance ($F_{(1,130)} = 0.528$, $p = 0.468$). Furthermore, from pre to post surgery (five-day average), stimulus lose-shift did not significantly differ in the sham condition ($T_{(8)} = 0.451$, $p = 0.664$) but did in the injury ($T_{(12)} = 2.955$, $p = 0.012$). Figure 3G and 3H illustrates this stimulus lose-shift data. Taken together, these results suggest that the injured condition had an increase in stimulus lose-shift strategy usage on PAL as a result of TBI. Sex did not affect any strategy usage, either pre or post injury, and did not interact with condition ($p > 0.05$, $\beta < 0.1$ for all measures).

3.2 iPAL Performance

After reaching PAL criterion post-surgery, both conditions were then tested on iPAL, a modification of PAL created to assess vulnerability to interference. This variation of PAL allowed us to infer executive dysfunction related to attentional deficits as measured through

the rodents' engagement with a task-irrelevant stimulus that never elicited reward. Figure 4A shows the average percent correct across 12 testing days. A LMEM fitting percent correct on iPAL with condition and day as fixed effects and subject as a random effect did not find the conditions statistically different (condition: $F_{(1,12.35)} = 0.975$, $p = 0.342$, day: $F_{(1,119)} = 0.596$, $p = 0.442$, interaction: $F_{(1,119)} = 1.290$, $p = 0.258$). Additionally, adding sex to the model did not account for any additional variance ($F_{(1, 9.058)} = 0.351$, $p = 0.568$, standardized $\beta = 0.06$). Figure 4B shows the cumulative error that occurred across 12 days of iPAL testing. The sham condition had an average of 331.3 ± 53.65 S.E.M errors. The injury condition had an average of 422.4 ± 35.01 S.E.M. An unpaired t-test did not find these conditions statistically different ($T_{(9)} = 1.469$, $p = 0.176$).

To quantify susceptibility to the maple leaf distractor, we evaluated novelty bias by calculating the ratio of [number of maple leaf touches in a session / number of trials in a session]. The average across the 12-testing days of iPAL for each condition is depicted in Figure 4C. The difference in the conditions was not significant ($t_{(8)} = 1.659$, $p = 0.136$). In iPAL, two types of errors can be made: interference error (error made by selecting the irrelevant distractor, i.e., novelty bias) and associative error (error unrelated to the distractor, the only error seen in standard PAL). Figure 4D shows the linear regression of these two types of errors as a proportion of the total error made on iPAL across the 12 testing days. A LMEM was fit for the difference between the two proportions across the 12 testing days with condition and day as fixed effects and animal as a random effect. This model found no significant effects of condition, ($F_{(1, 58.14)} = 1.255$, $p = 0.267$), day ($F_{(1, 119)} = 0.961$, $p = 0.329$), or condition by day interaction ($F_{(1, 119)} = 0.645$, $p = 0.423$). These results suggest that each condition experienced a similar proportion of error type on iPAL. Visualized another way, Figure 4E shows the error proportions as a function of the overall error rate on iPAL as an average across the 12 testing days. It is apparent that each error type makes up approximately half of the total error for both conditions. Finally, Figure 4F shows the error rates for both conditions averaged across the first 12 days of testing on PAL versus iPAL. To compare the error rates between PAL and iPAL, a 2-way ANOVA with PAL and iPAL error rates as a within subjects' factor and injury condition as a between subjects' factor revealed a main effect of PAL versus iPAL ($F_{(1,9)} = 42.76$, $p = 0.0001$) but no effect of condition ($F_{(1,9)} = 2.689$, $p = 0.136$) nor interaction between condition and PAL/iPAL error rates ($F_{(1,9)} = 0.465$). Taken together, these results suggest that the overall error rate for both conditions on iPAL was due to a similar proportion of associative and interference errors, and that both conditions exhibited additional error on iPAL that was interference related.

3.3 Spared Tissue Volume

During tissue processing, variability in lesion volume was qualitatively observed. While some CCI-injured rats had noticeable lesions and tissue loss, others had tissue swelling around the injury region. Figure 5A–D shows Nissl-stained tissue sections from four rats that were representative of the injury (Figure 5A and 5B) and sham (Figure 5C and 5D) conditions. Three different quantitative measurements of spared tissue around the injury site were taken for each rat as outlined in section 2.3. With subject variability accounted for in the LMEM, we found significant effects of condition ($F_{(1,10)} = 8.74$, $p = 0.014$), spared tissue volume measurement ($F_{(2,20)} = 1021$, $p < 0.0001$), and condition by volume

measurement interaction ($F_{(2,20)} = 7.863$, $p = 0.003$) in the spared tissue assessments. The addition of sex to the model did not explain any additional variance ($p > 0.05$, $\beta < 0.1$ for all measures). Figure 5E shows the quantifications of spared tissue volume. Overall spared tissue volume (normalized to contralateral hemisphere) was significantly different between group ($T_{(10)} = 3.027$, $p = 0.013$), as well as cortical spared volume ($T_{(10)} = 3.019$, $p = 0.013$), but hippocampal spared volume was insignificant ($T_{(10)} = 0.249$, $p = 0.808$). While we have reported normalized tissue volume to control for variability in brain size, please note that the group mean (across all 8 slices representing the extent of the injury region) for the CCI group was $98288462 \pm 8996758 \mu\text{m}^2$ and the group mean for the sham group was $106289876 \pm 8153694 \mu\text{m}^2$. Finally, the F -statistic of variance for the overall spared tissue volume was insignificant ($F_{(6,4)} = 0.197$).

3.4 Semiquantitative immunochemistry

Immunochemistry was performed on the tissue to assess the presence of GFAP and IBA1 antibody signal in the predefined 12 regions of interest, both ipsilateral and contralateral to the side of injury. Figure 6A–C shows microcopy images taken at 10X of the GFAP staining in three injured (A–C) and one sham (D) rat. Figure 6E shows 20X magnification images of the regions outlined in panel A. Figure 6F–G shows the quantification of GFAP optical density between conditions in the ipsilateral ROIS, between conditions in the contralateral ROIs, and ipsilateral versus contralateral side within the injury condition, respectively. LMEM was fit with condition, regions, and side as fixed effects, and subject as a random effect. This model revealed significant main effects of condition ($F_{(1,10.00)} = 7.336$, $p = 0.022$) and region ($F_{(11,229.00)} = 11.016$, $p < 0.0001$). Furthermore, there were significant interaction effects of condition by region ($F_{(11,229.1)} = 1.888$, $p = 0.042$), condition by side ($F_{(1,229.006)} = 29.773$, $p < 0.0001$), and condition by region by side ($F_{(11,229.00)} = 1.832$, $p = 0.050$). When sex was added to the model, it did not account for any additional variance ($p = 0.322$, $\beta = 0.07$).

Further two-way ANOVAs were run for GFAP optical density. Both ipsilateral hippocampal and thalamic ROIs had a significant main effect of condition (hippocampus: $F_{(1,50)} = 31.64$, $p < 0.0001$; thalamus: $F_{(1,70)} = 32.85$, $p < 0.0001$). Ipsilateral thalamus ROIs also had a significant effect region ($F_{(6,70)} = 2.944$, $p = 0.0128$), but the interaction between condition and region was not significant ($p = 0.173$). Ipsilateral hippocampal ROIs had no other significant effects ($p > 0.05$). Both contralateral hippocampal and thalamic ROIs had a significant main effect of condition (hippocampus: $F_{(1,50)} = 27.71$, $p < 0.0001$; thalamus: $F_{(1,70)} = 4.265$, $p = 0.043$), but no other effects ($p > 0.05$). Finally, within our injury condition, ANOVA revealed significant main effects of both side and region for hippocampus and thalamus (hpc: $F_{(1,60)} = 7.757$, $p = 0.007$, $F_{(4,60)} = 3.797$, $p = 0.008$; thal: $F_{(1,84)} = 29.67$, $p < 0.0001$, $F_{(6,84)} = 3.101$, $p = 0.009$). The interaction between side and region in the thalamic ROIs reached significance $F_{(6,84)} = 2.447$, $p = 0.031$, but became nonsignificant when adjusted for multiple comparisons.

Figure 7A–C shows microcopy images taken at 10X of the IBA1 staining in three injured (A–C) and one sham (D) rat. Figure 7E shows 20X magnification images of the regions outlined in panel A. Figure 7F–H shows the quantification of IBA1 optical density between

conditions in the ipsilateral ROIs, between conditions in the contralateral ROIs, and ipsilateral versus contralateral side within the injury condition, respectively. LMEM was fit with condition, regions, and side as fixed effects, and subject as a random effect. This model revealed a significant main effect of region ($F_{(11,230)} = 33.89$, $p < 0.0001$). Furthermore, there were significant interactions of condition by region ($F_{(11,230)} = 2.267$, $p = 0.012$), and condition by side ($F_{(1,230)} = 10.76$, $p = 0.001$). Unexpectedly, when sex was added to the model, there was a significant main effect of sex ($F_{(1,8)} = 6.154$, $p = 0.03807$), as well as an interaction between condition and sex ($F_{(1,8)} = 10.6994$, $p = 0.01134$). While the main effect does not reach significance after correction, the interaction does. However, because we are not sufficiently powered to detect sex differences (sham females $n=2$), we cannot make any conclusionary remarks. Nonetheless, this may be an interesting avenue to pursue in the future regarding sex differences in IBA1 expression following TBI.

Further two-way ANOVAs were run for IBA1 optical density. Ipsilateral thalamic, but not ipsilateral hippocampal, ROIs had a significant main effect of condition ($F_{(1,70)} = 19.54$, $p < 0.0001$). No other effects were found for ipsilateral ROIs between conditions ($p > 0.05$). Furthermore, contralateral thalamic, but not contralateral hippocampal, ROIs had a significant main effect of condition ($F_{(1,70)} = 13.90$, $p = 0.0004$). Ipsilateral thalamic ROIs also had a main effect of region ($F_{(6,70)} = 2.237$, $p = 0.049$), but the interaction between condition and region was nonsignificant when adjusted for multiple comparisons ($F_{(6,70)} = 2.237$, $p = 0.049$). There were no other effects ($p > 0.05$) for contralateral ROIs between conditions. Within our injury condition, ANOVA did not reveal any significant effects of contralateral/ipsilateral side, region, or their interaction for the hippocampal ROIs ($p > 0.05$ for all measures). For the thalamic ROIs, ANOVA revealed only a significant main effect of side ($F_{(1,84)} = 7.109$, $p = 0.009$).

3.5 Principal Component Analysis

Principal component analysis (PCA) was used as a dimensionality reduction technique on the variables obtained in this study to simplify correlational results and interpretation. PCAs were performed separately for the PAL behavioral data and the histological data. For the behavior, only PAL measures were included, as no conclusive effects of injury condition were found for iPAL. For each animal, behavioral measures included the average percent correct, location bias, stimulus bias, and stimulus lose-shift index for the first five days of PAL as well as the number of errors made until criterion was met. Only the first component of this analysis had an eigenvalue above 1. This component explained over 88% of the variance in the dataset, with each of the five measures loading comparably between $|0.38-0.48|$. Of note, percent correct had a positive loading and each of the other four performance measures loaded negatively, exemplifying a prior known relationship (Smith, Zequeira et al., 2022). Component scores for each animal were then taken from this component for subsequent correlation analysis.

For the histological data, measures for each animal included an average of the optical density across ROIs for the following significant ANOVAs (as shown in Figures 6 and 7): GFAP ipsilateral hippocampus, GFAP contralateral hippocampus, GFAP ipsilateral thalamus, IBA1 ipsilateral thalamus, & IBA1 contralateral thalamus. Spared tissue volume

measurements for the cortex and hippocampus were also included to encompass the spread of data that contributed to the significant hemisphere volume analysis. This analysis produced three components with an eigenvalue above 1. The first principal component had high loadings for the GFAP staining and accounted for 42.05% of the total variance. The second principal component had high loadings for the IBA1 staining and accounted for 28.18% of the total variance. The third component corresponded to the spared tissue volume of the hippocampus and cortex. This component explained 16.20% of the total variance. Together, these three components explained over 82% of the variance in this data set. Table 1 shows the variable loadings for these three components. As with the behavioral PCA, the component scores for each animal across these three components were taken for subsequent correlation analysis. A graphical depiction of the component dimensions and clustering seen with this analysis is depicted in Figure 8.

Taking the 4 component scores obtained for each animal (1 behavioral and 3 histological), we calculated Pearson's correlation coefficients (Table 2). This analysis revealed a significant correlation between the PAL behavior and histology component 2, which corresponded to IBA1 staining in the thalamus ($r = 0.83$, $p = 0.0008$). Furthermore, there was also a significant correlation between histology component 3, which corresponded to spared tissue volume, and histology component 1, which corresponded to GFAP staining ($r = 0.602$, $p = 0.039$). When accounting for multiple comparisons, however, the adjusted p-value is nonsignificant. Finally, the IBA1 and GFAP components displayed a highly significant correlation ($r = 0.990$, $p < 0.0001$). This was expected, but it is particularly noteworthy these highly correlated components did not display the same correlation to the PAL behavior (Fisher z-transformation; $Z_{(12)} = 1.733$, $p = 0.08$.)

4. DISCUSSION

The current *preliminary* study reports the deficits observed on a clinically relevant behavioral task, Paired Associates Learning (PAL), in a rat controlled cortical impact (CCI) model of traumatic brain injury (TBI). *The goal of this study was to employ trial-by-trial (TxT) behavioral analyses across the daily PAL testing sessions to carefully detail the behavioral phenotypes associated with cognitive dysfunction after CCI in rats. Automated, touchscreen-based cognitive testing in preclinical settings such as PAL provide researchers with a vast array of behavioral data that can be analyzed to provide more information regarding performance than task accuracy alone. While the main goal of this study was to employ these TxT behavioral analyses to better inform the extent of cognitive impairments after TBI in our model, postmortem histology was also implemented to quantify GFAP/IBA1 immunolabeling and spared tissue volume.* Principal component analysis was also used for dimension reduction to further understand the relations between the histological markers of TBI and the behavioral measurements obtained during PAL testing. Despite qualitative variability in tissue loss and immunostaining following TBI (Figures 5–7), PAL performance was found to decline in the injury condition after CCI compared to the sham condition (Figure 3A–C). *We also found that compared to sham, the CCI group had significant stimulus and location biases during PAL testing that were not present pre-surgery (Figure 3E–F). Furthermore, the CCI rodents were not more susceptible to irrelevant distractors than sham, as evidenced by testing the rodents on interference PAL*

(iPAL; Figure 4). Finally, after reducing several PAL performance measures into a single principal component and the histological measures into three principal components, there was a significant correlation of the rats' component scores between the PAL behavior and the principal component related to thalamic IBA1 staining in the histology (Figure 8).

TBI may severely affect cognitive processing. Traditionally, preclinical models assessing rodent cognition after modeling TBI have used assessments such as the Barnes Maze (Vink et al. 2003), fear conditioning (Sierra-Mercado et al. 2015), the Morris Water Maze (Xiong et al. 2012), and novel object recognition (Baratz et al. 2011). From these studies, it is clear that TBI can result in an array of cognitive dysfunction ranging from spatial working memory to nonspatial learning and recognition. However, studies assessing cognitive outcome more than 1 month after injury have been limited and many studies report no difference between injury and sham conditions at this chronic time point (Gold et al. 2013). More complex tasks that require a higher mental load, the integration of cognitive modalities, and are more homologous to clinical testing used in humans may be better suited to assess the long-term impacts of TBI on cognitive function.

The results from the present study validate previous findings from human study participants that PAL is sensitive to detecting cognitive impairment after TBI (Newcomb et al. 2011; De Simoni et al. 2016). Furthermore, our detailed analysis of behavioral deficits on PAL post-TBI compliments a recent study in rats using PAL as a cognitive training paradigm after TBI (Braeckman et al. 2020). Although they did not report a direct comparison of TBI versus control on PAL accuracy, and only included female rats, Braeckman et al. (2020) found that cognitive training on PAL increased microstructural organization in the hippocampus as measured by diffusion tensor imaging (DTI) metrics compared to no cognitive training. In our study, subcortical structures below the injured cortical region, namely a large portion of the hippocampus and midline thalamic nuclei, were shown to have accumulated protein markers of inflammatory processes after TBI. *The hippocampus is required for associative learning (Suzuki 2005), and for the PAL task specifically (Talpos et al. 2009; Langston et al. 2010; Yoon et al. 2012; Kim et al. 2015). Furthermore, several thalamic nuclei are densely reciprocally connected to the hippocampus and likely interact with medial temporal structures to support associative learning (Savage, Hall, & Vetreno 2011; Perry et al. 2018; Sziklas & Petrides 1999) and other forms of higher order cognition. There is a variety of literature to suggest that blood brain barrier dysfunction is prominent after TBI and may largely affect the thalamus (Ramlackhansingh et al. 2011; Vliet et al. 2020). Furthermore, circulating GFAP and IBA1 levels may be associated with pathophysiological sequelae in the thalamus of a pig model of mild TBI (Lafrenaye et al. 2020). While controlling neuroinflammation appears to be a strong candidate for TBI therapeutics, some current anti-inflammatory treatments have demonstrated little to no cognitive benefits in clinical testing (Homsy et al. 2009; Kelso et al. 2011; Ding et al. 2014). Although IBA1 staining does not provide sufficient analysis of inflammatory response to TBI nor justify the mechanisms that are responsible for the deficits seen in the PAL task, our findings that PAL task performance significantly correlated with IBA1 staining underscores PAL as a well-suited task for preclinical testing of anti-inflammatory interventions for treating cognitive dysfunction following TBI.*

The current study has several limitations and interpretation of these preliminary results should be made within the appropriate context. *First, the controlled cortical impact model of TBI used in this study involves a non-clinically relevant craniotomy and not all human TBIs are characterized by contusion (Osier and Dixon 2016). Therefore, the CCI model may not fully reflect all injuries seen in the human population. Future studies may benefit from the use of injury models which use blast force or rotational acceleration to simulate combat injuries such as the closed head model of engineered rotational acceleration (CHIMERA; Harr et al. 2019; McNamara et al. 2020). The behavioral analysis employed here for CCI may be especially useful for parsing apart subtle differences in deficits arising from CCI versus CHIMERA injuries.* Second, while we did assess the extent of lesion volume through the analysis of spared tissue, other studies have shown that structural white matter damage after TBI can reflect neurological outcomes (Kinnunen et al. 2011; Newcombe et al. 2016; Braun et al. 2017). Braeckman et al. (2020) showed that DTI metrics were a reliable measure to evaluate cognitive training in their rat model of TBI. Employing DTI with the TxT analysis of PAL deficits in this study will be a promising avenue for relating white matter damage to cognitive deficits post-TBI. Moreover, our study was not designed to have consistent endpoints for all rats. Some rats took longer to complete PAL than others, and thus the time from post-surgery to sacrifice differed slightly between rats. Future studies using this model will benefit from a time-restricted analysis of neuroinflammatory markers after TBI. *Finally, we were not sufficiently powered to detect sex differences, though we reported the addition of sex to our LMEMs. It is notable, however, that a power analysis indicated that 198 animals of each sex would be necessary to reject the null hypothesis of no sex differences in PAL performance with 80% probability.*

5. CONCLUSIONS

Understanding the complexities of TBI requires an evolving and reciprocal relationship between basic, translational, and clinical biomedical research. The development of automated touchscreen testing not only affords researchers a range of detailed behavioral data to assess performance more accurately on cognitive tasks, but also gives translational research the power to test methods of intervention in clinically relevant settings. This study found PAL task performance to decline after a unilateral parietal lobe impact that resulted in greater than expected injury variation, emphasizing PAL as a useful tool for testing the efficacy of interventions in preclinical models of TBI. *This manuscript also provided a TxT analysis of behavioral phenotypes during PAL testing, such as the tendency of a rodent to perseverate on an incorrect selection while performing the task. The successful treatment of TBI will likely rely upon individualized therapies that take into consideration the variety of factors that can influence positive treatment outcomes. The thorough behavioral analyses presented here for the PAL task may be useful for unpacking individual differences during intervention testing for TBI, and future studies evaluating TBI treatment efficacy in preclinical settings may benefit from using the TxT PAL analysis scripts provided with this manuscript.*

Acknowledgements:

This research was funded by the McKnight Brain Research Foundation Institute, the Department of Defense GRANT11811993 for the impact of PERK on post-traumatic tauopathy in Alzheimer's disease (JA), NIA R01AG049722/2RF1AG049722 (SNB), and the University of Florida Summer Neuroscience Internship Program (SMS). The authors would like to thank Aleyna Ross for the PAL graphic, Sarah Johnson and Sabrina Zequeira for the development of the iPAL task, and Wonn Pyon for helpful analytical discussion.

References

1. Acosta SA, Diamond DM, Wolfe S, Tajiri N, Shinozuka K, Ishikawa H, Hernandez DG, Sanberg PR, Kaneko Y, & Borlongan CV (2013). Influence of post-traumatic stress disorder on neuroinflammation and cell proliferation in a rat model of traumatic brain injury. *PLoS One*, 8(12), e81585. doi: 10.1371/journal.pone.0081585 [PubMed: 24349091]
2. Baratz R, Tweedie D, Rubovitch V, Luo W, Yoon JS, Hoffer BJ, Greig NH, & Pick CG (2011). Tumor necrosis factor- α synthesis inhibitor, 3,6'-dithiothalidomide, reverses behavioral impairments induced by minimal traumatic brain injury in mice. *J Neurochem*, 118(6), 1032–1042. doi:10.1111/j.1471-4159.201107377.x [PubMed: 21740439]
3. Barr DJ, Levy R, Scheepers C, & Tily HJ (2013). Random effects structure for confirmatory hypothesis testing: Keep it maximal. *J Mem Lang*, 68(3). doi: 10.1016/j.jml.2012.11.001
4. Borgens RB, & Liu-Snyder P (2012). Understanding secondary injury. *Q Rev Biol*, 87(2), 89–127. doi: 10.1086/665457 [PubMed: 22696939]
5. Braeckman K, Descamps B, Vanhove C, & Caeyenberghs K (2020). Exploratory relationships between cognitive improvements and training induced plasticity in hippocampus and cingulum in a rat model of mild traumatic brain injury: a diffusion MRI study. *Brain Imaging Behav*, 14(6), 2281–2294. doi: 10.1007/s11682-019-00179-4 [PubMed: 31407153]
6. Braun M, Vaibhav K, Saad NM, Fatima S, Vender JR, Baban B, Hoda MN, & Dhandapani KM (2017). White matter damage after traumatic brain injury: A role for damage associated molecular patterns. *Biochim Biophys Acta Mol Basis Dis*, 1863(10 Pt B), 2614–2626. doi:10.1016/j.bbadis.2017.05.020 [PubMed: 28533056]
7. Brown VA (2021). An Introduction to Linear Mixed-Effects Modeling in R. *Advances in Methods and Practices in Psychological Science*, 4(1), 2515245920960351. doi: 10.1177/2515245920960351
8. Bussey TJ, Padain TL, Skillings EA, Winters BD, Morton AJ, & Saksida LM (2008). The touchscreen cognitive testing method for rodents: how to get the best out of your rat. *Learn Mem*, 15(7), 516–523. doi: 10.1101/lm.987808 [PubMed: 18612068]
9. Centers for Disease Control and Prevention (2022). Surveillance Report of Traumatic Brain Injury-related Deaths by Age Group, Sex, and Mechanism of Injury—United States, 2018 and 2019. Centers for Disease Control and Prevention, U.S. Department of Health and Human Services.
10. Collie A, Myers C, Schnirman G, Wood S, & Maruff P (2002). Selectively impaired associative learning in older people with cognitive decline. *J Cogn Neurosci*, 14(3), 484–492. doi: 10.1162/089892902317361994 [PubMed: 11970807]
11. Cusimano MD, Saarela O, Hart K, Zhang S, & McFaul SR (2020). A population-based study of fall-related traumatic brain injury identified in older adults in hospital emergency departments. *Neurosurg Focus*, 49(4), E20. doi:10.3171/2020.7.FOCUS20520
12. De Simoni S, Grover PJ, Jenkins PO, Honeyfield L, Quest RA, Ross E, Scott G, Wilson MH, Majewska P, Waldman AD, Patel MC, & Sharp DJ (2016). Disconnection between the default mode network and medial temporal lobes in post-traumatic amnesia. *Brain*, 139(Pt 12), 3137–3150. doi:10.1093/brain/aww241 [PubMed: 27797805]
13. Ding K, Wang H, Xu J, Li T, Zhang L, Ding Y, Zhu L, He J, & Zhou M (2014). Melatonin stimulates antioxidant enzymes and reduces oxidative stress in experimental traumatic brain injury: the Nrf2-ARE signaling pathway as a potential mechanism. *Free Radic Biol Med*, 73, 1–11. doi:10.1016/j.freeradbiomed.2014.04.031 [PubMed: 24810171]
14. Diwadkar VA, Flaughner B, Jones T, Zalanyi L, Ujfalussy B, Keshavan MS, & Erdi P (2008). Impaired associative learning in schizophrenia: behavioral and computational studies. *Cogn Neurodyn*, 2(3), 207–219. doi:10.1007/s11571-008-9054-0 [PubMed: 19003486]

15. Giunta B, Obregon D, Velisetty R, Sanberg PR, Borlongan CV, & Tan J (2012). The immunology of traumatic brain injury: a prime target for Alzheimer's disease prevention. *J Neuroinflammation*, 9, 185. doi:10.1186/1742-2094-9-185 [PubMed: 22849382]
16. Gold EM, Su D, López-Velázquez L, Haus DL, Perez H, Lacuesta GA, Anderson AJ, & Cummings BJ (2013). Functional assessment of long-term deficits in rodent models of traumatic brain injury. *Regen Med*, 8(4), 483–516. doi:10.2217/rme.13.41 [PubMed: 23826701]
17. Hausmann ON (2003). Post-traumatic inflammation following spinal cord injury. *Spinal Cord*, 41(7), 369–378. doi:10.1038/sj.sc.3101483 [PubMed: 12815368]
18. Hickman DL, & Swan M (2010). Use of a body condition score technique to assess health status in a rat model of polycystic kidney disease. *J Am Assoc Lab Anim Sci*, 49(2), 155–159. [PubMed: 20353688]
19. Homsí S, Federico F, Croci N, Palmier B, Plotkine M, Marchand-Leroux C, & Jafarian-Tehrani M (2009). Minocycline effects on cerebral edema: relations with inflammatory and oxidative stress markers following traumatic brain injury in mice. *Brain Res*, 1291, 122–132. doi:10.1016/j.brainres.2009.07.031 [PubMed: 19631631]
20. Jurga AM, Paleczna M, & Kuter KZ (2020). Overview of General and Discriminating Markers of Differential Microglia Phenotypes. *Front Cell Neurosci*, 14, 198. doi:10.3389/fncel.2020.00198 [PubMed: 32848611]
21. Kelso ML, Scheff NN, Scheff SW, & Pauly JR (2011). Melatonin and minocycline for combinatorial therapy to improve functional and histopathological deficits following traumatic brain injury. *Neurosci Lett*, 488(1), 60–64. doi:10.1016/j.neulet.2010.11.003 [PubMed: 21056621]
22. Kim CH, Heath CJ, Kent BA, Bussey TJ, & Saksida LM (2015). The role of the dorsal hippocampus in two versions of the touchscreen automated paired associates learning (PAL) task for mice. *Psychopharmacology (Berl)*, 232(21–22), 3899–3910. doi:10.1007/s00213-015-3949-3 [PubMed: 25963561]
23. Kinnunen KM, Greenwood R, Powell JH, Leech R, Hawkins PC, Bonnelle V, Patel MC, Counsell SJ, & Sharp DJ (2011). White matter damage and cognitive impairment after traumatic brain injury. *Brain*, 134(Pt 2), 449–463. doi:10.1093/brain/awq347 [PubMed: 21193486]
24. Kramer ME, Chiu CY, Shear PK, & Wade SL (2009). Neural correlates of verbal associative memory and mnemonic strategy use following childhood traumatic brain injury. *J Pediatr Rehabil Med*, 2(4), 255–271. doi:10.3233/PRM-2009-0091 [PubMed: 21188286]
25. Kuznetsova A, Brockhoff PB, & Christensen RHB (2017). lmerTest Package: Tests in Linear Mixed Effects Models. *Journal of Statistical Software*, 82(13), 1–26. doi:10.18637/jss.v082.i13
26. Lafrenaye AD, Mondello S, Wang KK, Yang Z, Povlishock JT, Gorse K, Walker S, Hayes RL, & Kochanek PM (2020). Circulating GFAP and Iba-1 levels are associated with pathophysiological sequelae in the thalamus in a pig model of mild TBI. *Sci Rep*, 10(1), 13369. doi:10.1038/s41598-020-70266-w [PubMed: 32770054]
27. Langston RF, & Wood ER (2010). Associative recognition and the hippocampus: differential effects of hippocampal lesions on object-place, object-context and object-place-context memory. *Hippocampus*, 20(10), 1139–1153. doi:10.1002/hipo.20714 [PubMed: 19847786]
28. Lee A, Archer J, Wong CK, Chen SH, & Qiu A (2013). Age-related decline in associative learning in healthy Chinese adults. *PLoS One*, 8(11), e80648. doi:10.1371/journal.pone.0080648 [PubMed: 24265834]
29. McAllister TW, & Arciniegas D (2002). Evaluation and treatment of postconcussive symptoms. *NeuroRehabilitation*, 17(4), 265–283. [PubMed: 12547976]
30. McNamara EH, Grillakis AA, Tucker LB, & McCabe JT (2020). The closed-head impact model of engineered rotational acceleration (CHIMERA) as an application for traumatic brain injury pre-clinical research: A status report. *Exp Neurol*, 333, 113409. doi:10.1016/j.expneurol.2020.113409 [PubMed: 32692987]
31. Mishra AM, Bai X, Sanganahalli BG, Waxman SG, Shatillo O, Grohn O, Hyder F, Pitkanen A, & Blumenfeld H (2014). Decreased resting functional connectivity after traumatic brain injury in the rat. *PLoS One*, 9(4), e95280. doi:10.1371/journal.pone.0095280 [PubMed: 24748279]
32. Newcombe VF, Correia MM, Ledig C, Abate MG, Outtrim JG, Chatfield D, Geeraerts T, Manktelow AE, Garyfallidis E, Pickard JD, Sahakian BJ, Hutchinson PJ, Rueckert D, Coles JP,

- Williams GB, & Menon DK (2016). Dynamic Changes in White Matter Abnormalities Correlate With Late Improvement and Deterioration Following TBI: A Diffusion Tensor Imaging Study. *Neurorehabil Neural Repair*, 30(1), 49–62. doi:10.1177/1545968315584004 [PubMed: 25921349]
33. Ohsawa K, Imai Y, Sasaki Y, & Kohsaka S (2004). Microglia/macrophage-specific protein Iba1 binds to fimbrin and enhances its actin-bundling activity. *J Neurochem*, 88(4), 844–856. doi:10.1046/j.1471-4159.2003.02213.x [PubMed: 14756805]
34. Osier N, & Dixon CE (2016). The Controlled Cortical Impact Model of Experimental Brain Trauma: Overview, Research Applications, and Protocol. *Methods Mol Biol*, 1462, 177–192. doi:10.1007/978-1-4939-3816-2_11 [PubMed: 27604719]
35. Perry BAL, Mercer SA, Barnett SC, Lee J, & Dalrymple-Alford JC (2018). Anterior thalamic nuclei lesions have a greater impact than mammillothalamic tract lesions on the extended hippocampal system. *Hippocampus*, 28(2), 121–135. doi:10.1002/hipo.22815 [PubMed: 29150979]
36. Quinn DK, Mayer AR, Master CL, & Fann JR (2018). Prolonged Postconcussive Symptoms. *Am J Psychiatry*, 175(2), 103–111. doi:10.1176/appi.ajp.2017.17020235 [PubMed: 29385828]
37. Ramlackhansingh AF, Brooks DJ, Greenwood RJ, Bose SK, Turkheimer FE, Kinnunen KM, Gentleman S, Heckemann RA, Gunanayagam K, Gelosa G, & Sharp DJ (2011). Inflammation after trauma: microglial activation and traumatic brain injury. *Ann Neurol*, 70(3), 374–383. doi:10.1002/ana.22455 [PubMed: 21710619]
38. Robbins TW, James M, Owen AM, Sahakian BJ, McInnes L, & Rabbitt P (1994). Cambridge Neuropsychological Test Automated Battery (CANTAB): a factor analytic study of a large sample of normal elderly volunteers. *Dementia*, 5(5), 266–281. doi:10.1159/000106735 [PubMed: 7951684]
39. Savage LM, Hall JM, & Vetreno RP (2011). Anterior thalamic lesions alter both hippocampal-dependent behavior and hippocampal acetylcholine release in the rat. *Learn Mem*, 18(12), 751–758. doi: 10.1101/lm.023887.111 [PubMed: 22086393]
40. Sierra-Mercado D, McAllister LM, Lee CC, Milad MR, Eskandar EN, & Whalen MJ (2015). Controlled cortical impact before or after fear conditioning does not affect fear extinction in mice. *Brain Res*, 1606, 133–141. doi:10.1016/j.brainres.2015.02.031 [PubMed: 25721797]
41. Silver JM, Koumaras B, Chen M, Mirski D, Potkin SG, Reyes P, Warden D, Harvey PD, Arciniegas D, Katz DI, & Gunay I (2006). Effects of rivastigmine on cognitive function in patients with traumatic brain injury. *Neurology*, 67(5), 748–755. doi:10.1212/01.wnl.0000234062.98062.e9 [PubMed: 16966534]
42. Silver JM, Koumaras B, Meng X, Potkin SG, Reyes PF, Harvey PD, Katz DI, Gunay I, & Arciniegas DB (2009). Long-term effects of rivastigmine capsules in patients with traumatic brain injury. *Brain Inj*, 23(2), 123–132. doi:10.1080/02699050802649696 [PubMed: 19191091]
43. Smith SM, Zequeira S, Ravi M, Johnson SA, Hampton AM, Ross AM, Pyon W, Maurer AP, Bizon JL, & Burke SN (2022). Age-related impairments on the touchscreen paired associates learning (PAL) task in male rats. *Neurobiol Aging*, 109, 176–191. doi:10.1016/j.neurobiolaging.2021.09.021 [PubMed: 34749169]
44. Suzuki WA (2007). Making new memories: the role of the hippocampus in new associative learning. *Ann N Y Acad Sci*, 1097, 1–11. doi:10.1196/annals.1379.007 [PubMed: 17413005]
45. Sziklas V, & Petrides M (1999). The effects of lesions to the anterior thalamic nuclei on object-place associations in rats. *Eur J Neurosci*, 11(2), 559–566. doi:10.1046/j.1460-9568.1999.00448.x [PubMed: 10051755]
46. Taffe MA, Weed MR, Gutierrez T, Davis SA, & Gold LH (2002). Differential muscarinic and NMDA contributions to visuo-spatial paired-associate learning in rhesus monkeys. *Psychopharmacology (Berl)*, 160(3), 253–262. doi:10.1007/s00213-001-0954-5 [PubMed: 11889494]
47. Talpos JC, Winters BD, Dias R, Saksida LM, & Bussey TJ (2009). A novel touchscreen-automated paired-associate learning (PAL) task sensitive to pharmacological manipulation of the hippocampus: a translational rodent model of cognitive impairments in neurodegenerative disease. *Psychopharmacology (Berl)*, 205(1), 157–168. doi:10.1007/s00213-009-1526-3 [PubMed: 19357840]

48. Ullman-Culleré MH, & Foltz CJ (1999). Body condition scoring: a rapid and accurate method for assessing health status in mice. *Lab Anim Sci*, 49(3), 319–323. [PubMed: 10403450]
49. van Vliet EA, Ndode-Ekane XE, Lehto LJ, Gorter JA, Andrade P, Aronica E, Grohn O, & Pitkanen A (2020). Long-lasting blood-brain barrier dysfunction and neuroinflammation after traumatic brain injury. *Neurobiol Dis*, 145, 105080. doi:10.1016/j.nbd.2020.105080 [PubMed: 32919030]
50. Vink R, Young A, Bennett CJ, Hu X, Connor CO, Cernak I, & Nimmo AJ (2003). Neuropeptide release influences brain edema formation after diffuse traumatic brain injury. *Acta Neurochir Suppl*, 86, 257–260. doi:10.1007/978-3-7091-0651-8_55 [PubMed: 14753447]
51. Vonder Haar C, Martens KM, Bashir A, McInnes KA, Cheng WH, Cheung H, Stukas S, Barron C, Ladner T, Welch KA, Crompton PA, Winstanley CA, & Wellington CL (2019). Repetitive closed-head impact model of engineered rotational acceleration (CHIMERA) injury in rats increases impulsivity, decreases dopaminergic innervation in the olfactory tubercle and generates white matter inflammation, tau phosphorylation and degeneration. *Exp Neurol*, 317, 87–99. doi:10.1016/j.expneurol.2019.02.012 [PubMed: 30822421]
52. Weed MR, Taffe MA, Polis I, Roberts AC, Robbins TW, Koob GF, Bloom FE, & Gold LH (1999). Performance norms for a rhesus monkey neuropsychological testing battery: acquisition and long-term performance. *Brain Res Cogn Brain Res*, 8(3), 185–201. doi:10.1016/s0926-6410(99)00020-8 [PubMed: 10556598]
53. Yoon J, Seo Y, Kim J, & Lee I (2012). Hippocampus is required for paired associate memory with neither delay nor trial uniqueness. *Learn Mem*, 19(1), 1–8. doi:10.1101/lm.024554.111 [PubMed: 22174309]

HIGHLIGHTS

- PAL performance declines in a rat model of TBI.
- Response-driven bias in PAL becomes elevated after TBI.
- Inflammatory microglial response in the thalamus correlates with PAL deficit.

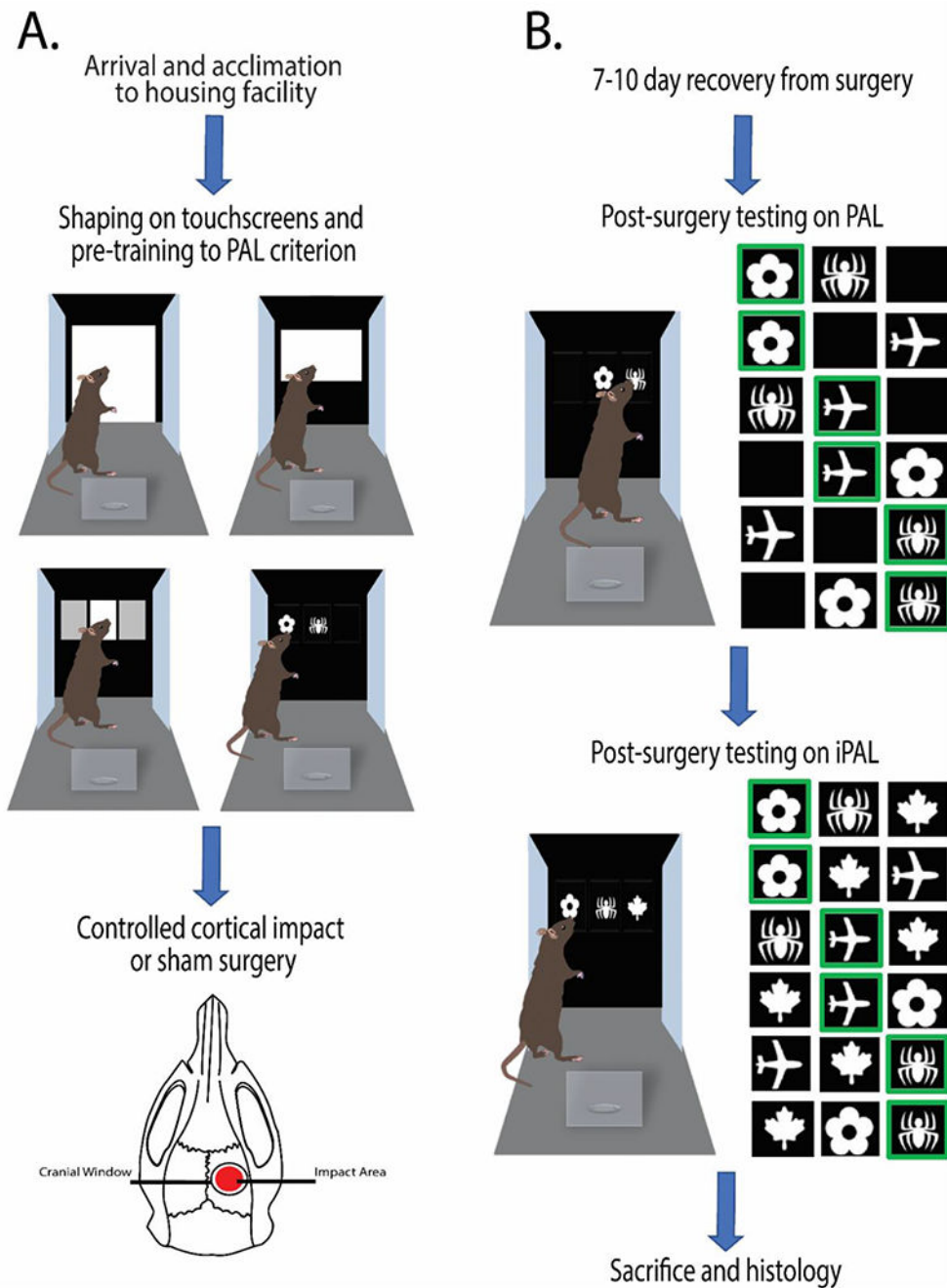


Figure 1. Schematic of experimental timeline.

A) Pre-surgical experimental timeline. Rats were incrementally shaped to engage with the touchscreen chambers and pre-trained to reach PAL criterion. Following criterion achievement, rats were pseudo randomly selected for either CCI or sham surgery. **B)** Post-surgical experimental timeline. After a 7-10 day recovery from surgery, rodents were re-tested on PAL until criterion was met. Upon achievement of criterion, rats were tested for 12 days on iPAL. After completion of all behavior testing, animals were transcardially perfused for postmortem histological analysis.

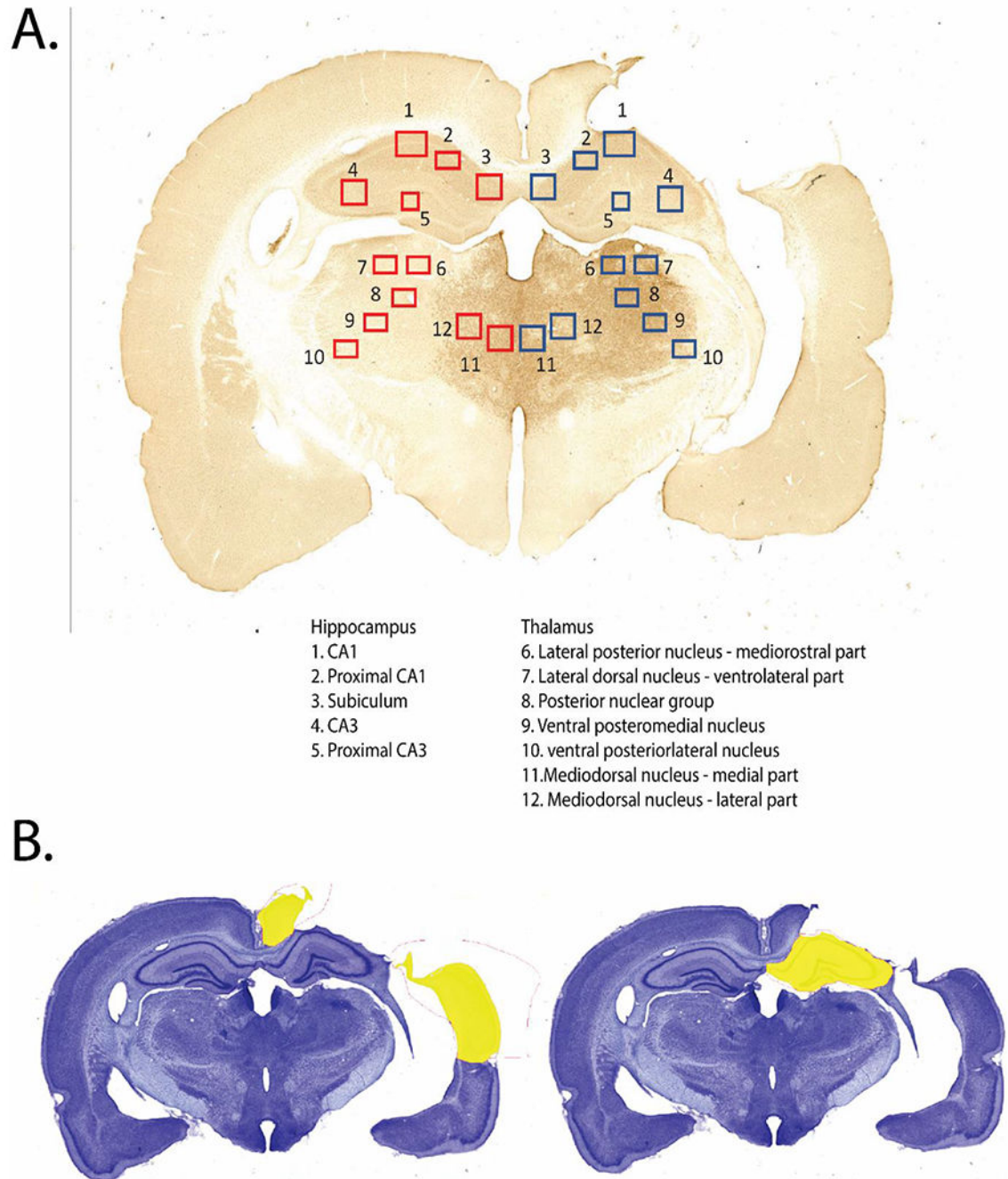


Figure 2. Depiction of parameters for postmortem histological analysis.

A) IBA1 stained section for a CCI rat with the 12 regions of interest identified for analysis superimposed on the ipsilateral (dark blue) and contralateral (red) hemispheres. **B)** Images of nissl-stained sections from a *male* CCI rat highlighting spared lesion volume tracings (yellow) for the cortex (left) and hippocampus (right).

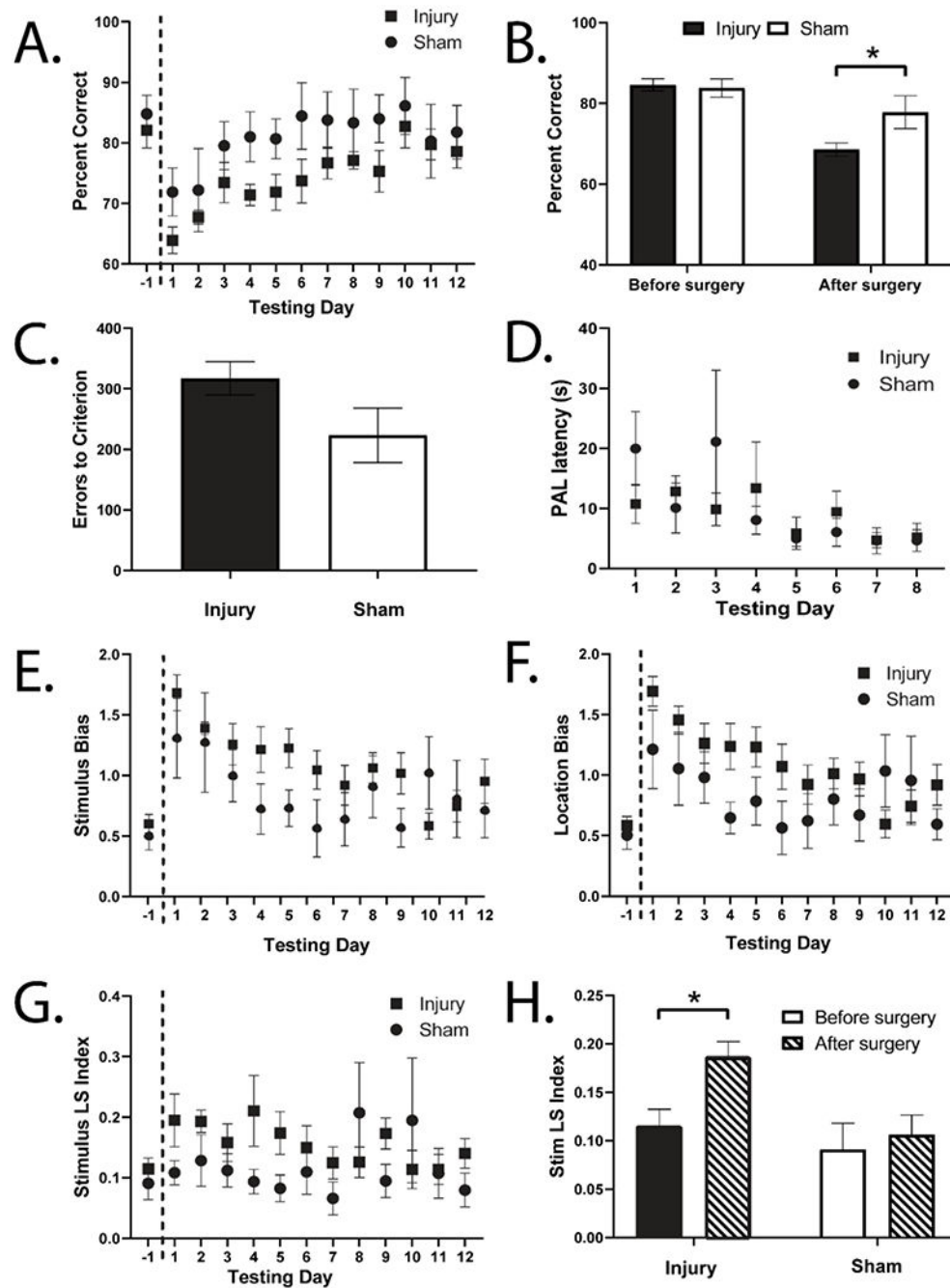


Figure 3. CCI resulted in PAL performance deficits compared to sham condition.

A) Post-surgical PAL performance was significantly affected by injury condition and day of testing, as well an interaction between the two as measured by percent correct ($p < 0.05$ for all measures). **B)** Before surgery, both conditions performed comparably on PAL. After surgery, injury condition had significantly reduced percent correct ($p < 0.05$). **C)** After surgery, injured rats trended toward having more errors on PAL prior to reaching criterion ($p < 0.1$). **D)** There was no effect of injury condition on PAL trial latency after surgery. **E)** Post-surgical stimulus bias on PAL was significantly affected by injury condition ($p < 0.05$) and an interaction

between day and injury condition ($p < 0.01$). **F**) Post-surgical location bias on PAL was significantly affected by injury condition ($p < 0.01$) as well as an interaction between day and injury condition ($p < 0.001$). **G**) Post-surgical stimulus lose-shift index on PAL was significantly affected by injury condition ($p < 0.01$) as well as an interaction between day and injury condition ($p < 0.05$). **H**) Injury condition showed a significant increase in stimulus lose-shift index from pre to post-surgery ($p < 0.05$), but sham condition did not.

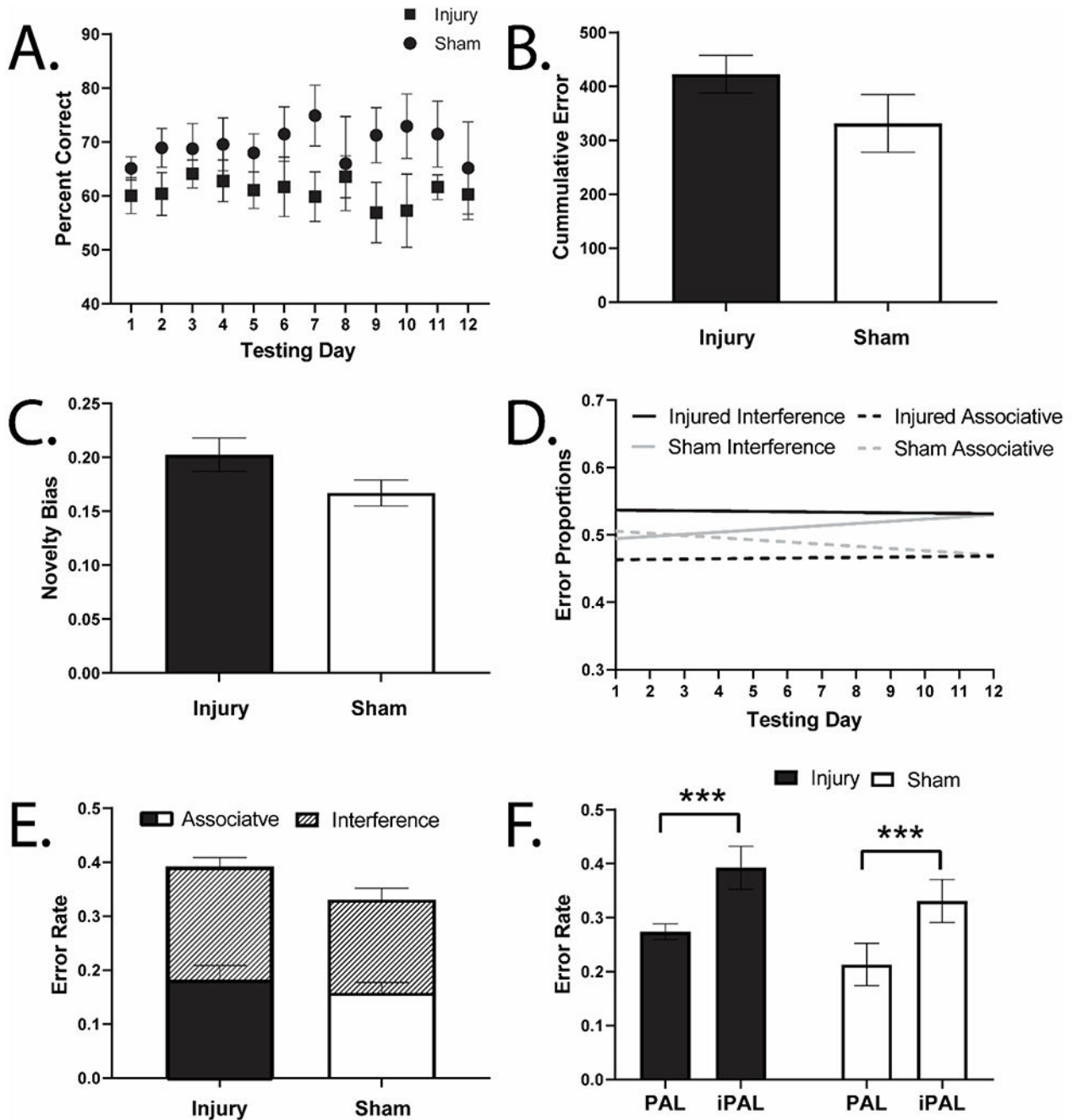


Figure 4. CCI did not result in statistically significant iPAL performance deficits compared to sham condition.

A) Post-surgical iPAL performance was not significantly affected by injury condition, day, or condition by day interaction ($p > 0.05$). **B)** Injury condition showed a trend toward more errors on iPAL ($p < 0.2$) with modest effect size. **C)** Injury condition showed a trend toward more interference errors as measured by novelty bias (maple leaf touches /total trials) ($p < 0.2$). **D & E)** Both injury and sham conditions showed similar proportions of error type across

iPAL testing ($p > 0.05$). **F**) Both injury and sham conditions showed increased error rate from PAL to iPAL ($p < 0.0001$).

Author Manuscript

Author Manuscript

Author Manuscript

Author Manuscript

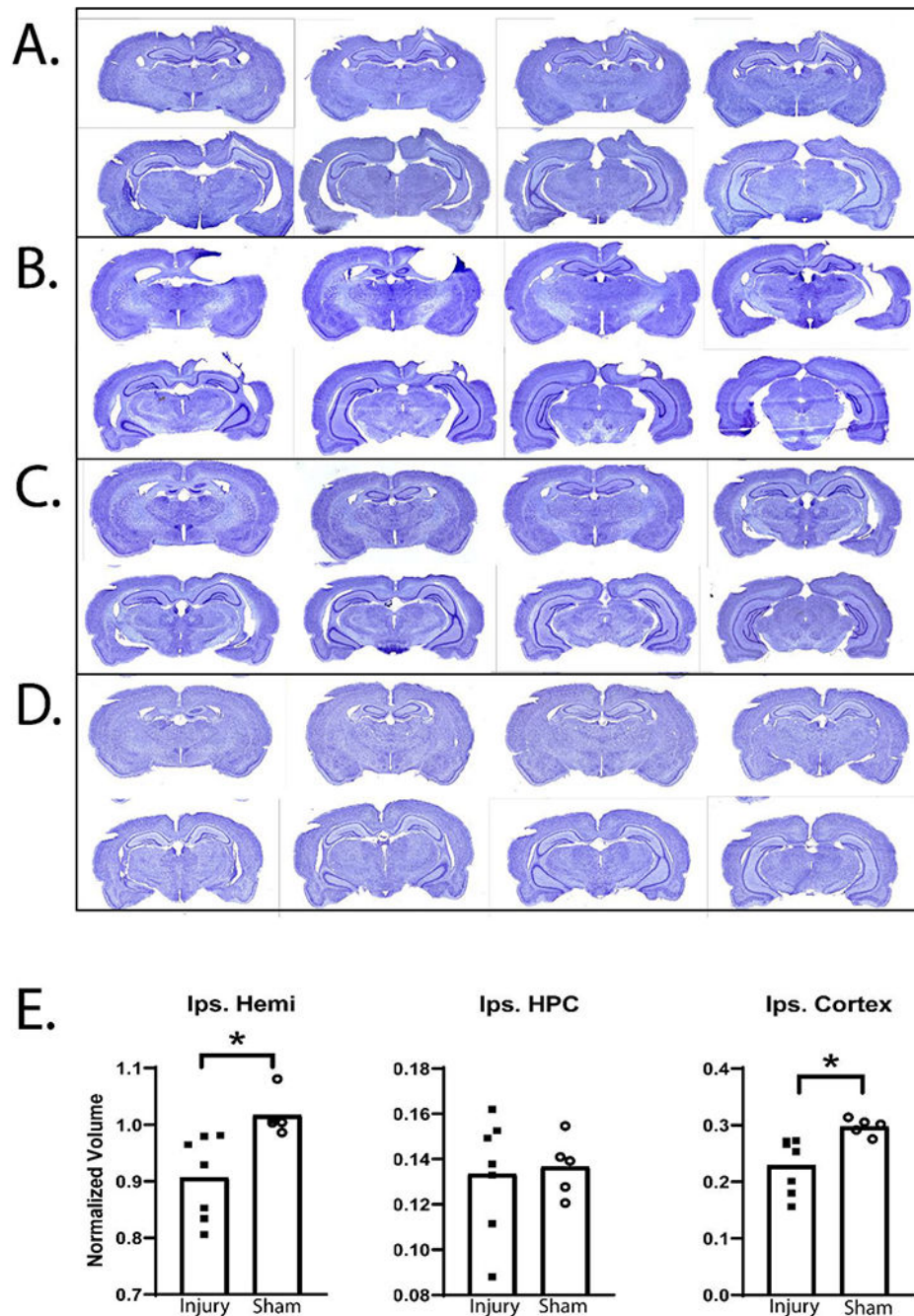


Figure 5. CCI resulted in greater tissue loss compared to sham condition as measured by spared tissue volume.

A-D) Nissl-stained sections across extent of injury for two different *male* CCI rats (**A,B**) and two different *male* sham rats (**C,D**). Qualitative variability in lesion volume between CCI rats can be seen by the different patterns of injury exhibited in the sections of rat A versus rat B. **E)** CCI rats had lower spared tissue volume compared to sham in the hemisphere ipsilateral to injury site (left; $p < 0.01$). Separating the measurements into hippocampal

(middle) or cortical (right) spared volume, injured animals only differed from sham in spared cortical volume ($p < 0.05$).

Author Manuscript

Author Manuscript

Author Manuscript

Author Manuscript

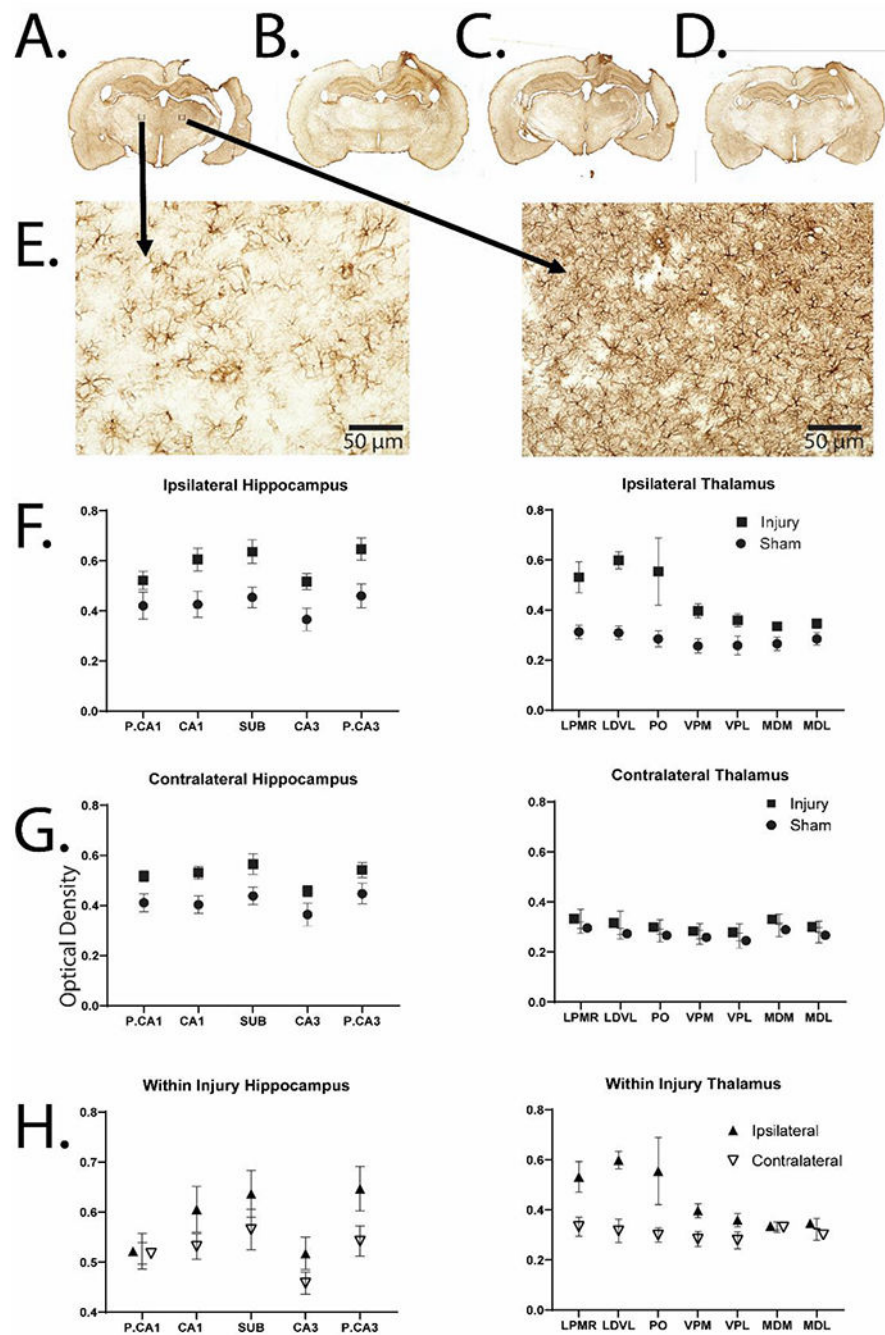


Figure 6. CCI resulted in elevated GFAP staining as measured by optical density compared to sham condition.

A-D) 10X stitched images of GFAP stained sections for 3 different CCI rats (A-C) and 1 sham rat (D). **E)** 20X images taken from the regions defined in panel A. **F)** CCI resulted in greater optical density of GFAP in the side ipsilateral to the injury site compared to sham. Both hippocampus (left) and thalamus (right) had significant effects of condition ($p < 0.0001$). **G)** CCI resulted in greater optical density of GFAP in the side contralateral to injury site compared to sham in the hippocampus only ($p < 0.01$). **F)** Within the CCI

condition, rats had greater optical density of GFAP on the side ipsilateral to injury for both hippocampus (left; $p < 0.01$) and thalamus (right; $p < 0.0001$) ROIs.

Author Manuscript

Author Manuscript

Author Manuscript

Author Manuscript

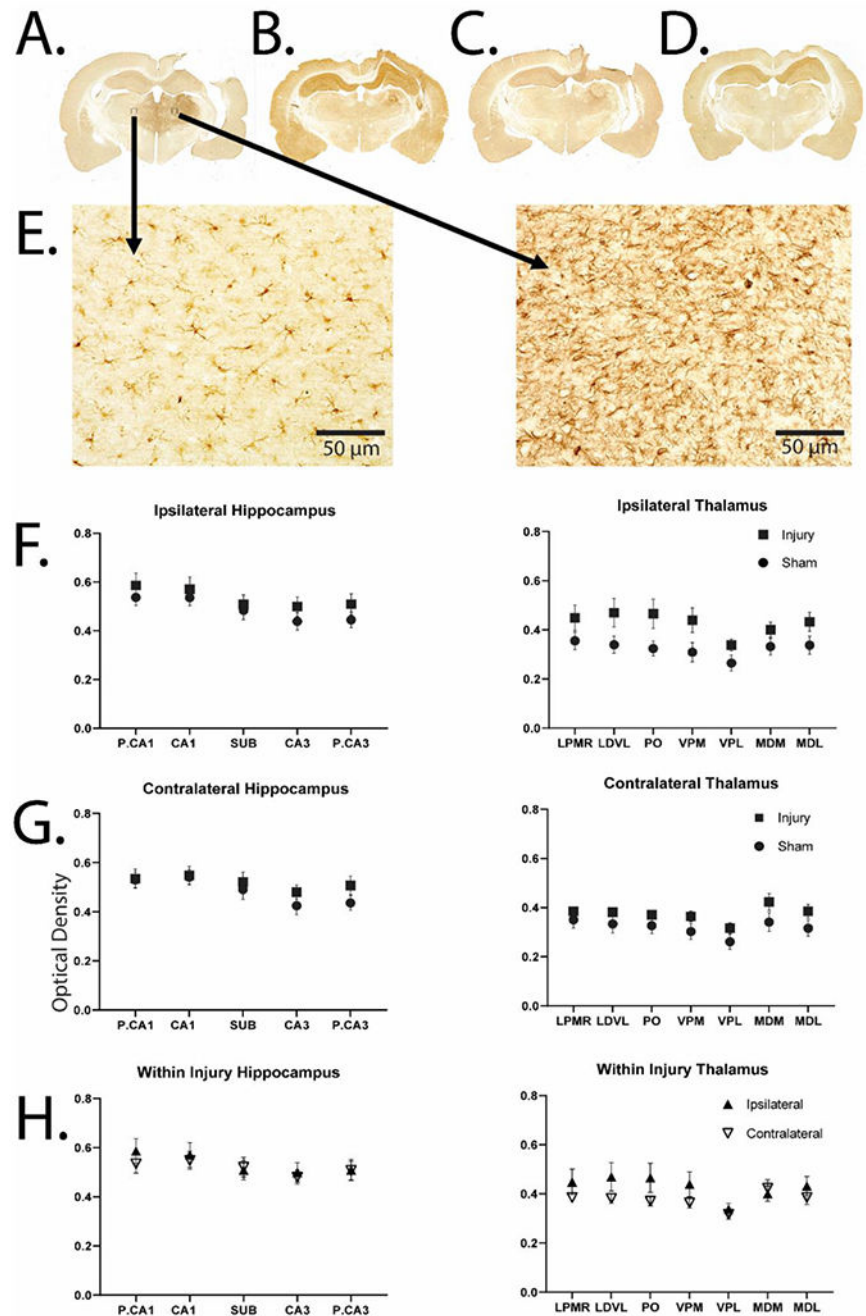


Figure 7. CCI resulted in elevated IBA1 staining as measured by optical density compared to sham condition.

A-D) 10X stitched images of IBA1 stained sections for 3 different CCI rats (A-C) and 1 sham rat (D). **E)** 20X images taken from the regions defined in panel A. **F)** CCI resulted in greater optical density of IBA1 in the side ipsilateral to injury site only in the thalamic ROIS ($p < 0.0001$). **G)** CCI resulted in greater optical density of IBA1 in the side contralateral to injury site only in the thalamic ROIS ($p < 0.001$). **H)** Within the CCI condition, rats had a

greater optical density of IBA1 on the side ipsilateral to injury for only the thalamic ROIs ($p < 0.01$).

Author Manuscript

Author Manuscript

Author Manuscript

Author Manuscript

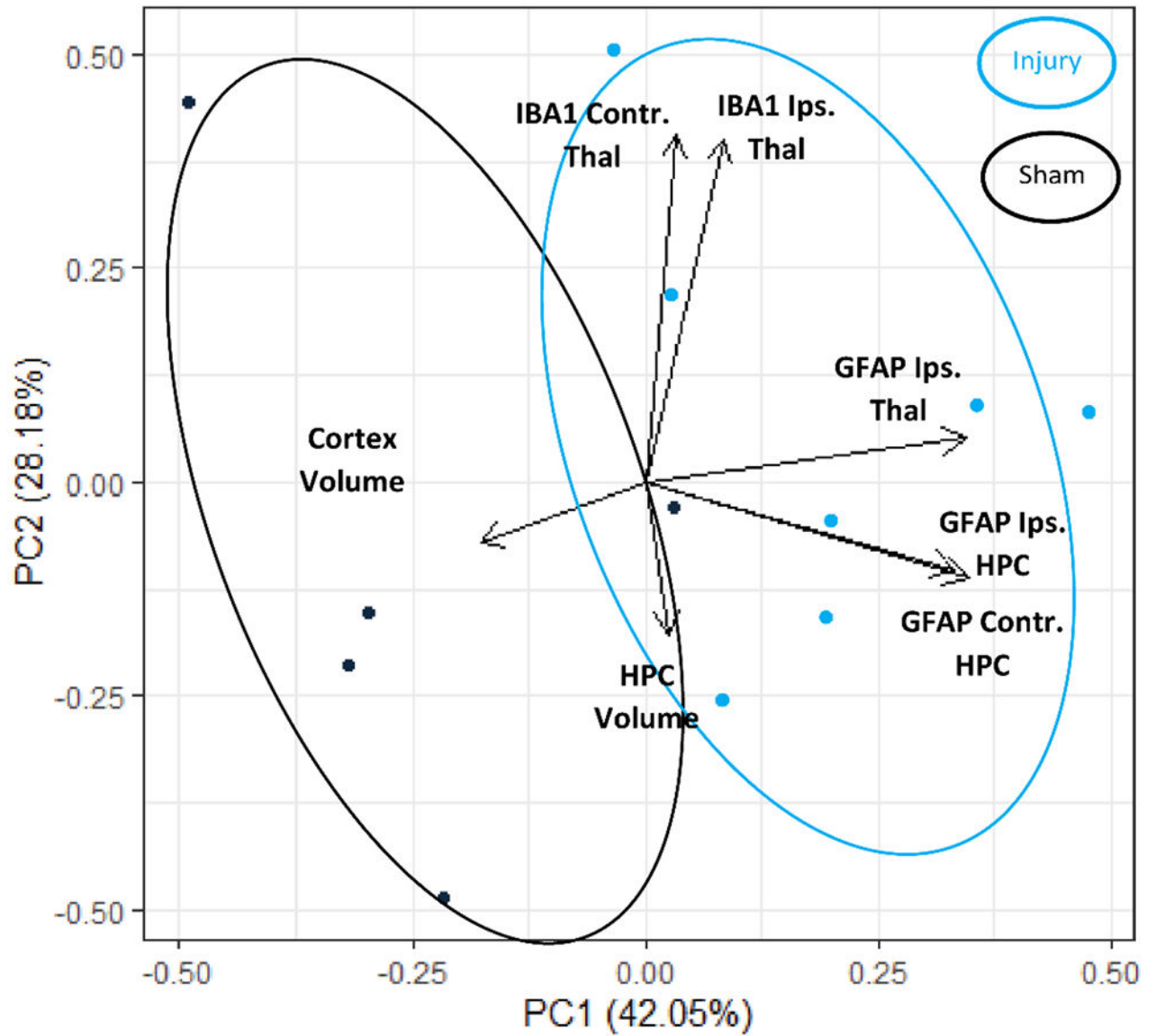


Figure 8. Graphical representation of the component dimensions and clustering for the histology PCA analysis.

Although the model was naïve to injury condition, the histology PCA clustered CCI and sham animals into two distinct groups. Three components above an eigenvalue of 1 were found.

Table 1.
Loading values for the seven variables of the histology PCA analysis.

Component 1 (42.05% of variance) corresponded to GFAP staining as indicated by the high loadings for the three GFAP variables, component 2 (28.18% of variance) corresponded to IBA1 staining, and component 3 (16.2% of variance) corresponded to spared tissue volume. Only loadings above 0.4 are depicted.

Variables	Component 1 (42.05%)	Component 2 (28.18%)	Component 3 (16.20%)
GFAP Ipsilateral Hippocampus	0.556		
GFAP Contralateral Hippocampus	0.531		
GFAP Ipsilateral Thalamus	0.552		
IBA1 Ipsilateral Thalamus		0.643	
IBA1 Contralateral Thalamus		0.652	
Hippocampal Spared Volume			0.697
Cortex Spared Volume			0.612

Table 2.
Pearson's correlation coefficients for the four PCA components (one behavior and three histology).

PAL behavior was highly correlated with IBA1 staining in the thalamus ($p < 0.001$). Spared tissue volume was moderately correlated with GFAP staining, but was statistically nonsignificant after correction for multiple comparisons ($p > 0.05$). IBA1 and GFAP components were extremely correlated ($p < 0.0001$), and it is noteworthy that these highly correlated components did not display the same correlation to PAL behavior ($p = 0.08$).

	PAL Behavior Component 1	Histology Component 1	Histology Component 2	Histology Component 3
PAL Behavior Component 1		0.3575	0.8309	0.2569
Histology Component 1	0.3575		0.9899	0.6017
Histology Component 2	0.8309	0.9899		0.0926
Histology Component 3	0.2569	0.6017	0.0926	